

HRC-I/*Chandra* X-ray observations towards σ Orionis

J. A. Caballero^{1,2}, J. F. Albacete-Colombo³, and J. López-Santiago²

¹ Centro de Astrobiología (CSIC-INTA), Carretera de Ajalvir km 4, 28850 Torrejón de Ardoz, Madrid, Spain

² Departamento de Astrofísica y Ciencias de la Atmósfera, Facultad de Física, Universidad Complutense de Madrid, 28040 Madrid, Spain

³ Centro Universitario Regional Zona Atlántica, Universidad Nacional del Comahue, Monseñor Esandi y Ayacucho, 8500 Viedma, Río Negro, Argentina

Received 25 April 2010 / Accepted 11 Jun 2010

ABSTRACT

Aims. We investigated the X-ray emission from young stars and brown dwarfs in the σ Orionis cluster ($\tau \sim 3$ Ma, $d \sim 385$ pc) and its relation to mass, presence of circumstellar discs, and separation to the cluster centre by taking advantage of the superb spatial resolution of the *Chandra* X-ray Observatory.

Methods. We used public HRC-I/*Chandra* data from a 97.6 ks pointing towards the cluster centre and complemented them with X-ray data from IPC/*Einstein*, HRI/*ROSAT*, EPIC/*XMM-Newton*, and ACIS-S/*Chandra* together with optical and infrared photometry and spectroscopy from the literature and public catalogues. On our HRC-I/*Chandra* data, we measured count rates, estimated X-ray fluxes, and searched for short-term variability. We also looked for long-term variability by comparing with previous X-ray observations.

Results. Among the 107 detected X-ray sources, there were 70 cluster stars with known signposts of youth, two young brown dwarfs, 12 cluster member candidates, four field dwarfs, and two galaxies with optical-infrared counterpart. The remaining sources had extragalactic nature. Based on a robust Poisson- χ^2 analysis, nine cluster stars displayed flares or rotational modulation during the HRC-I observations, while other eight stars and one brown dwarf showed X-ray flux variations between the HRC-I and IPC, HRI, and EPIC epochs. We constructed a cluster X-ray luminosity function from O9.5 (about $18 M_{\odot}$) to M6.5 (about $0.06 M_{\odot}$). We found: (i) a tendency of early-type stars in multiple systems or with spectroscopic peculiarities to display X-ray emission, (ii) that the two detected brown dwarfs and the least-massive star are among the σ Orionis objects with the highest L_X/L_J ratios, and (iii) that a large fraction of known classical T Tauri stars in the cluster are absent in this and other X-ray surveys. Finally, from a spatial distribution analysis, we quantified the impact of the sensitivity degradation towards the HRC-I borders on the detection of faint X-ray sources, and concluded that dozens X-ray σ Orionis stars and brown dwarfs are still to be detected.

Key words. stars: brown dwarfs – stars: early-type – stars: flare – stars: variables: T Tauri, Herbig Ae/Be – Galaxy: open clusters and associations: individual: σ Orionis – X-ray: stars

1. Introduction

The Trapezium-like system σ Ori, the fourth brightest “star” in the Orion Belt, illuminates the Horsehead Nebula and injects energy into its homonymous cluster, σ Orionis (Garrison 1967; Wolk 1996; Béjar et al. 1999). Its age ($\tau \sim 3$ Ma – Zapatero Osorio et al. 2002; Sherry et al. 2004), relative closeness ($d \sim 385$ pc – Caballero 2008b; Mayne & Naylor 2008), low extinction ($0.04 \text{ mag} < E(B - V) < 0.09 \text{ mag}$ – Béjar et al. 2004; Sherry et al. 2008), and high spatial density (Caballero 2008a) make the cluster an ideal site to look for and characterise sub-stellar objects (Zapatero Osorio et al. 2000; Béjar et al. 2001; Caballero et al. 2007; Bihain et al. 2009). The cluster is also investigated, for example, to study circumstellar discs based on optical spectroscopy (Kenyon et al. 2005; Sacco et al. 2008; Gatti et al. 2008) or mid-infrared photometry (Oliveira et al.

2006; Caballero 2007a; Zapatero Osorio et al. 2008; Luhman et al. 2008) and young X-ray emitter stars (Sanz-Forcada et al. 2004; Franciosini et al. 2006; Skinner et al. 2008; López-Santiago & Caballero 2008 and references therein).

X-ray observations in young open clusters, such as σ Orionis, provide information on winds of early-type stars, high-temperature coronae of late-type stars, absorption by circumstellar discs, magnetic activity associated to fast rotation, the cluster X-ray luminosity function, and, in general, the evolution of young (pre-)main-sequence stars. Except for the *ROSAT* variability analysis in Caballero et al. (2009), the latest X-ray studies in σ Orionis have been carried out using instruments onboard the *XMM-Newton* and *Chandra* space missions. In this work, we analyse in detail observations of a large portion of the cluster accomplished with the *Chandra* High Resolution Camera (HRC). The lower sensitivity of HRC with respect to EPIC/*XMM-Newton* (European Photon Imaging Cameras) used by Franciosini et al. (2006) was compensated by the better spa-

Send offprint requests to: José Antonio Caballero, e-mail: caballero@cab.inta-csic.es

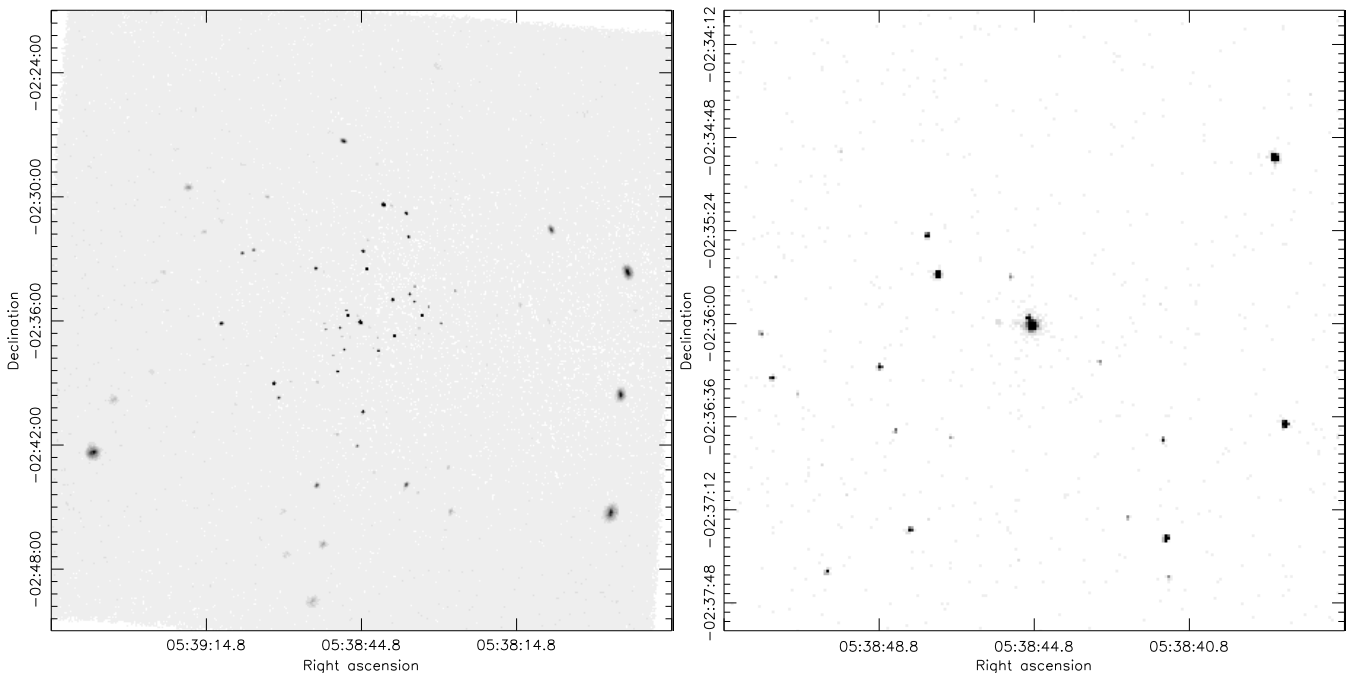


Fig. 1. HRC-I/*Chandra* images centred on σ Ori AB. Approximate sizes are 30×30 arcmin² (left; note the borders of the field of view in the corners) and 4×4 arcmin² (right; see also the Fig. 4 in Caballero 2007b). North is up, east is left.

tial resolution and a longer exposure time, of almost 100 ks. Besides, the HRC observations in σ Orionis were more sensitive and covered a larger field of view than those performed with ACIS/*Chandra* (Advanced CCD Imaging Spectrometer) by Skinner et al. (2008)¹. HRC observations provide, however, no spectral information.

Some preliminary results based on the HRC/*Chandra* dataset, which is publicly available from the *Chandra* Data Archive² since 2003, have been advanced by Adams et al. (2002, 2003, 2004, 2005) and Caballero (2005, 2007b). Here, we detect X-ray sources on the deep HRC image, cross-identify them with optical, near-infrared, and previously-known X-ray sources, classify them into young and field stars and galaxies using state-of-the-art spectro-, astro-, and photometric data, compare with previous X-ray observations, and study the X-ray luminosity function in the cluster, the frequency of X-ray emitters, and its relation to spatial location, disc occurrence, and stellar mass.

2. Analysis and results

2.1. Data retrieval

HRC, held in the *Chandra* focal plane array together with ACIS, is a double CsI-coated microchannel plate detector similar to the High Resolution Imaging photon-counting detectors onboard the *Einstein Observatory* and *ROSAT*. However, HRC has substantially increased capability compared with them in X-ray quantum efficiency (in the energy range 0.08–10.0 keV), detector size (90×90 mm² or 16 Mpx, which translates into a

field of view of 31×31 arcmin²), internal background rate, and, specially, spatial resolution (down to 0.016 arcsec).

Using the web version of ChaSeR at the *Chandra* Data Archive, we searched and retrieved the package of primary data products associated to the observations with identification number 2560 (sequence number 200168, principal investigator S. Wolk). Observations were carried out on 2002 Nov 21–22 and took a total exposure time of 97.6 ks. The field of view was approximately centred on σ Ori D (Mayrit 13084), a B2V star located at 13 arcsec to the massive binary (possibly triple) star σ Ori AB at the bottom of the gravitational well in the centre of the σ Orionis cluster.

2.2. Reduction

Data reduction, starting with the level-1 event list provided by the processing pipeline at the *Chandra* X-ray Center, was performed using the *Chandra* Interactive Analysis of Observations software CIAO 3.4³ and the *Chandra* Calibration Database CALDB 3.4.1⁴. We produced a level-2 event file using the CIAO task `hrc_process_events`. The data were filtered to remove events that did not have a good event “grade” or that had one or more of the “status bits” set to unity (see the definitions of “grade” and “status bits” at the *Chandra*/CIAO dictionary⁵). Intervals of solar background flaring were searched for, but none were found (see, however, Section 2.6). As a result, we assumed a constant background and did not applied time filtering. An exposure map, needed by the source detection algorithm and to re-normalise source count rates, was calculated with

¹ Skinner et al. (2008) also used the High Energy Transmission Grating, HETG, for the brightest sources.

² <http://cxc.harvard.edu/cda/>

³ <http://cxc.harvard.edu/ciao3.4/>

⁴ <http://cxc.harvard.edu/caldb3/>

⁵ <http://chandra.ledas.ac.uk/ciao/dictionary/>

the CIAO tool `mkexppmap` assuming a monochromatic spectrum ($k_B T = 1.0$ keV). See further details in Albacete-Colombo et al. (2008), where an alike reduction process was performed.

2.3. Source detection

Source detection was accomplished with the Palermo Wavelet Detection code `PWDetect`⁶ version 1.3.2 (Damiani et al. 1997a) on the level-2 event list restricted to the 0.5–10 keV energy band and specifically compiled to run for a maximum of 7×10^6 events. `PWDetect` analyses the data at different spatial scales, from 0.25 to 16 arcsec, allowing the detection of both point-like and moderately extended sources and the efficient resolution of close sources pairs. The most important input parameter required by the code is the final threshold significance for detection, S_{\min} (in equivalent Gaussian σ s), which depends on the background level, detector, and desired number of spurious detections per field due to Poisson noise, as determined from extensive simulations of source-free fields (cf. Damiani et al. 1997a). We determined the total number of background counts detected during the entire exposure over the full HRC-I detector at 4.5×10^6 photons with a proprietary IDL script. This background level translated into a final detection threshold of $S_{\min} = 5.1\sigma$ if we impose only *one spurious* detection in the field of view.

A total of 109 HRC-I sources with $S > 5.1\sigma$ were found with `PWDetect`. We visually inspected each X-ray source and identified two “double detections”, corresponding to the stars Mayrit 3020 AB (No. 25) and Mayrit 156353 (No. 11). In detail, for each optical counterpart, `PWDetect` revealed two X-ray sources, one bright and one faint and slightly decentered, separated by a few tens of arcsecond. This separation is smaller than the sizes of the point spread functions of the X-ray sources. The double detections may arise because of bad adopted background estimate near bright X-ray sources (Damiani et al. 1997a, 1997b). We discarded the faint X-ray sources in the two cases⁷ and kept the remaining 107 sources as reliable X-ray detections. Their coordinates, significances of detection (S), angular separations to the centre of field of view (offaxis), count rate, and associated uncertainties are listed in Table C.1. The sources are sorted by decreasing significance of detection.

In addition, we estimated the apparent X-ray flux⁸ for each source. We integrated the counts over a circular area three times wider than the one used by `PWDetect`, which is in turn smaller than the size of the local point spread function. More than 97 % of the photons of a source fall within the circular area. A mean background level was subtracted after integrating the counts over an area of the same radius (but free of X-ray emission)

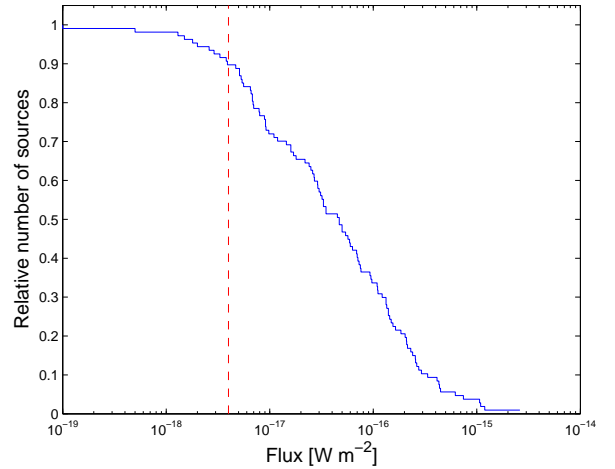


Fig. 2. Relative cumulative number of the HRC-I/*Chandra* X-ray sources as a function of apparent flux. The vertical [red] dashed line at $0.4 \times 10^{-17} \text{ W m}^{-2}$ indicates the approximate completeness flux of our survey.

in the vicinity of each source. Finally, for the conversion between counts and energy, we used the factor $\overline{E}_\gamma = 1.2$ keV (mean energy per X-ray photon), which is representative of late-type young stars in σ Orionis. This value was obtained by determining a weighted mean of the coronal temperatures of the stars in Table 3 in López-Santiago & Caballero (2008). The completeness flux limit, which marks an inflection point in the cumulative number of X-ray sources as a function of apparent flux, was $0.4 \times 10^{-17} \text{ W m}^{-2}$ (Fig. 2). The actual completeness limit varies with the offaxis separation (Section 3.4).

2.4. Cross-identification

We cross-matched the 107 X-ray sources in Table C.1 with optical and near-infrared catalogues. First, we searched for their optical/near-infrared counterparts in the Mayrit catalogue of young stars and brown dwarfs in the σ Orionis cluster (Caballero 2008c). He tabulated coordinates, $iJHK_s$ magnitudes (from the DENIS and 2MASS catalogues – Epchtein et al. 1997; Skrutskie et al. 2006), and youth features of a large number of confirmed and candidate cluster members. He also tabulated foreground field dwarfs and background galaxies. Of the 107 X-ray sources in our work, 77 were in the Mayrit catalogue. Secondly, we found the optical/near-infrared counterparts of other 13 X-ray sources not tabulated in the Mayrit catalogue, listed in Table 1. Caballero (2008c) did not record them because they had no 2MASS counterpart (Nos. 25 and 58) or known youth features at that time and were located bluewards of his conservative selection criterion in the i vs. $i - K_s$ diagram (the remaining 11 stars). However, most of the 11 “blue” X-ray stars are “red” enough to have been considered in previous photometric searches in the cluster (see references in footnote to Table 1).

In total, we found the optical/near-infrared counterparts of 90 X-ray sources. The separations between the coordinates of the 2MASS and our X-ray sources is plotted against the sepa-

⁶ http://www.astropa.unipa.it/progetti_ricerca/PWDetect/

⁷ We thank I. Pillitteri for helpful guidance in this subject.

⁸ Throughout this work, we use the word ‘flux’ for denoting the quantity λF_λ . For transforming between the Système international d’unités and the centimetre-gram-second system, use the conversion factor $10^{-14} \text{ erg cm}^{-2} \text{ s}^{-1} \equiv 10^{-17} \text{ W m}^{-2}$. Using $d = 385$ pc to the σ Orionis cluster, a flux $\mathcal{F} = 10^{-17} \text{ W m}^{-2}$ translates into a *cgs* luminosity $\log L_X \approx 29.25$.

Table 1. X-ray stars not tabulated in the Mayrit catalogue (Caballero 2008c)^a.

No.	Name	α (J2000)	δ (J2000)	i [mag]	J [mag]	H [mag]	K_s [mag]	References ^c
25	* Mayrit 3020 AB	05 38 44.84	-02 35 57.1	10.4±0.2	10.70±0.07	10.480±0.010	vLO03, Ca05, Bo09
31	* [W96] 4771-1056	05 39 00.52	-02 39 39.0	12.371±0.06	11.665±0.028	11.221±0.024	11.110±0.022	Wo96, Sk08
39	* Mayrit 168291 AB	05 38 34.31	-02 35 00.0	12.272±0.03	11.216±0.031	10.565±0.033	10.354±0.030	He07, Ga08, Sk08
46	Mayrit 1093033	05 39 24.56	-02 20 44.1	12.727±0.16	11.371±0.026	10.778±0.024	10.554±0.023	He07
47	* Mayrit 68229	05 38 41.35	-02 36 44.4	14.404±0.03	12.988±0.026	12.330±0.024	12.084±0.025	Wo96, Ca07b, Sk08
48	Mayrit 172264	05 38 33.35	-02 36 17.6	13.393±0.02	12.052±0.027	12.295±0.023	11.107±0.027	Sh04, Sk08
51	[SWW2004] 166	05 38 53.06	-02 38 53.6	12.717±0.02	11.625±0.026	11.034±0.026	10.828±0.025	Sh04, Ol06, Sk08
57	* Mayrit 492211	05 38 27.74	-02 43 00.9	13.636±0.03	11.189±0.030	11.447±0.024	10.287±0.024	Sh04, Sa08
58	* Mayrit 21023	05 38 45.31	-02 35 41.3	13.41±0.09	12.98±0.06	12.73±0.09	Ca07b, Bo09
85	Mayrit 270196	05 38 39.72	-02 40 19.7	15.489±0.05	13.746±0.031	13.099±0.026	12.883±0.028	Sk08
95 ^b	Mayrit 605079	05 39 24.35	-02 34 01.3	14.501±0.19	12.978±0.030	12.272±0.026	12.058±0.021	Sh04, Sa07, Sa08
98	Mayrit 1178039	05 39 33.78	-02 20 39.8	13.783±0.15	12.367±0.026	11.598±0.023	11.429±0.023	Sh04, Ol06
99	Mayrit 957055	05 39 37.29	-02 26 56.7	13.000±0.03	11.698±0.026	10.974±0.024	10.773±0.021	Sh04

^a Stars marked with an asterisk, ‘*’, are commented in Section B.1.

^b See Section 2.5.1 for a discussion on Mayrit 605079.

^c Reference abbreviations – Wo96: Wolk (1996); vLO03: van Loon & Oliveira (2003); Sh04: Sherry et al. (2004); Ca05: Caballero (2005); Ol06: Oliveira et al. (2006); Ca07b: Caballero (2007b); Sa07: Sacco et al. (2007); He07: Hernández et al. (2007); Ga08: Gatti et al. (2008); Sa08: Sacco et al. (2008); Sk08: Skinner et al. (2008); Bo09: Bouy et al. (2009).

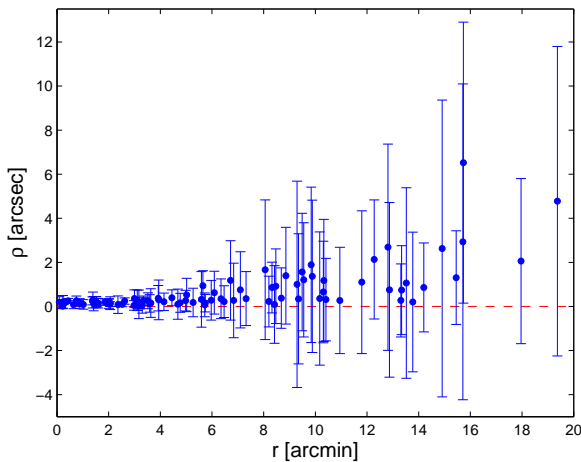


Fig. 3. Separation between the 90 correlated HRC-I sources and their 2MASS counterparts as a function of separation to the cluster centre (ρ vs. r diagram). The horizontal (red) dashed line marks $\rho = 0$ arcsec (all the data points are located above this line).

ration to the centre of the field of view in Fig. 3. None of them separates from zero by more than 1σ (accounting for the errors in the determination of the photo-centroids of the HRC-I and 2MASS sources). Average separations are $\Delta\alpha = 0.2 \pm 1.0$ arcsec and $\Delta\delta = 0.0 \pm 0.7$ arcsec. Square-mean-roots in the innermost 3 arcmin, where the HRC-I point spread functions are sharper, get below 0.1 arcsec.

The remaining 17 non-cross-matched X-ray sources and their closest 2MASS sources are listed in Table 2. Following

López-Santiago & Caballero (2008), we also looked for the optical photographic counterparts in the USNO-B1 catalogue (Monet et al. 2003). We had no success with the cross-matching. In all cases, the separations between the coordinates of the HRC-I and 2MASS sources are larger than 2σ and get larger than 6σ in 13 cases. These 13 HRC-I sources must have counterparts fainter than the USNO-B1, DENIS, and 2MASS limiting magnitudes at $B_J \sim 21.0$ mag, $R_F \sim 20.0$ mag, $i \sim 18.0$ mag, $J \sim 17.1$ mag, $H \sim 16.4$ mag, and $K_s \sim 14.3$ mag, respectively. We are not confident about the non-cross-matching of the other four X-ray sources, which are separated to their closest 2MASS sources by less than 3σ . In two cases, Nos. 62 and 96, nearby galaxies undetected by USNO-B1, DENIS, or 2MASS are visible in public images (see footnotes to Table 2). Finally, in the other two cases, Nos. 97 and 107, the errors in coordinates of X-ray sources could be underestimated and the 2MASS sources, which are cluster member candidates (Burningham et al. 2005; Caballero 2007b), may be the actual optical counterparts (note the small angular separation of No. 97).

2.5. Source classification

On the one hand, we have classified the 90 HRC-I sources with near-infrared counterpart into 84 young cluster members and candidates, four X-ray field stars, and two X-ray galaxies (Table C.2). Details on this classification are given next. On the other hand, the 13 HRC-I sources without optical or near-infrared counterparts at separations larger than 6σ are galaxies (possibly active galactic nuclei; López-Santiago & Caballero 2008). The remaining four sources without (or with questionable) counterpart seem to be two galaxies as well (Nos. 62

Table 2. The closest 2MASS sources to X-ray galaxy candidates without optical/near-infrared counterpart listed in Table C.1^a.

No.	α (J2000)	δ (J2000)	ρ [arcsec]	Name
24	05 38 35.10	−02 34 55.9	18.1	...
56	05 38 39.65	−02 30 21.0	13.9	[SWW2004] 79
62	* 05 38 14.22	−02 35 07.3	6.31	[W96] rJ053814
68	05 38 59.65	−02 38 15.6	41.2	...
76	05 38 53.37	−02 33 22.9	24.4	Mayrit 203039
83	05 38 59.22	−02 33 31.6	28.2	...
91	05 38 41.37	−02 28 31.8	12.3	...
93	* 05 38 44.70	−02 43 22.3	38.9	...
96	* 05 39 06.64	−02 38 08.1	3.22	...
97	* 05 38 43.86	−02 37 06.8	0.766	Mayrit 68191
100	05 38 24.49	−02 29 22.8	27.9	...
101	05 38 50.42	−02 36 43.1	11.5	...
102	05 38 42.00	−02 39 23.2	15.7	...
104	05 38 36.77	−02 42 54.6	13.7	...
105	05 38 34.79	−02 34 15.8	16.2	Mayrit 182305
106	05 39 10.21	−02 37 09.8	25.9	...
107	* 05 38 28.25	−02 32 27.4	4.16	[BNL2005] 1.02

^a Sources marked with an asterisk, “*”, are commented in Section B.2.

and 96; see above) and two cluster member candidates (Nos. 97 and 107). Given the reasonable uncertainty in the actual nature of the last four sources, we cautiously discarded them for next steps of the analysis. Colour-magnitude and colour-colour diagrams in Fig. 4 illustrate the source classification.

2.5.1. Cluster members and candidates

Of the 84 young cluster members and candidates, 72 (86 %) have uncontroversial features of youth: OB spectral type, intense Li I $\lambda 6707.8 \text{ \AA}$ resonant doublet in absorption, mid-infrared flux excess due to a circumstellar disc, strong (broad, asymmetrical) H α emission due to accretion, and/or weak alkali absorption lines due to low gravity (Caballero 2008c and references therein; González-Hernández et al. 2008; Sacco et al. 2008). Two of them are fainter than the star-brown boundary at $J \approx 14.5 \text{ mag}$ (Caballero et al. 2007) and are, therefore, *bona fide* X-ray “young brown dwarfs” (Section 3.3.2). The other 70 cluster members are classified in Table C.2 as “young stars”.

There remain 12 stars that follow the photometric sequence defined by the confirmed cluster stars in Fig. 4 and that we classify as “young star candidates”. All of them have been classified in the same way in other photometric (Wolk 1996; Sherry et al. 2004; Scholz & Eislöffel 2004; Caballero 2007b; Hernández et al. 2007; Bouy et al. 2009) and X-ray (Franciosini et al. 2006; Skinner et al. 2008) searches in the cluster. Of the young star candidates, there is spectroscopic information only for one. Mayrit 605079 (No. 95, [SWW2004] 127), a photo-

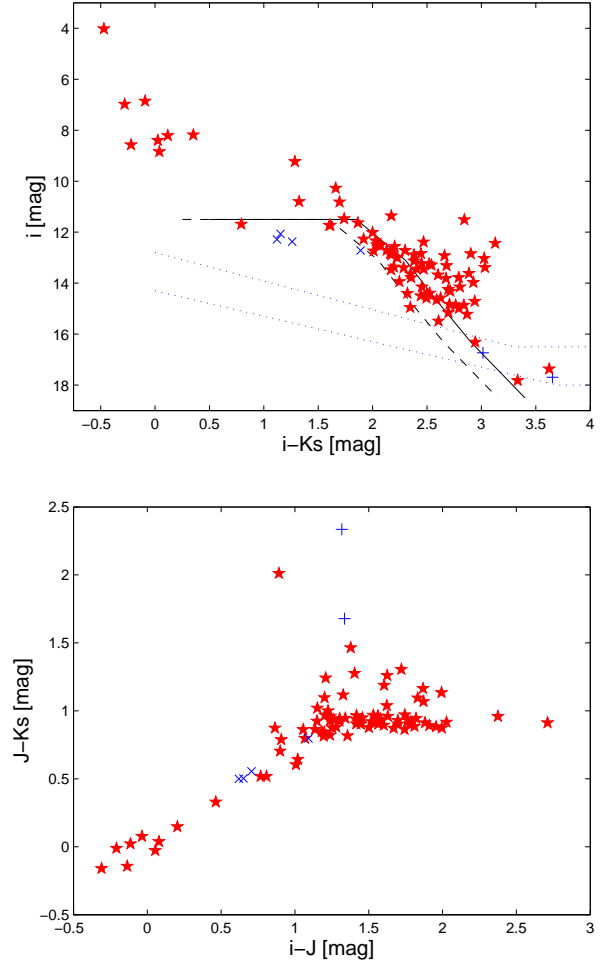


Fig. 4. Colour-magnitude and colour-colour diagrams. The different symbols represent: cluster star and brown dwarf members and candidates (red filled stars); field stars (blue crosses), and galaxies (blue pluses). In the i vs. $i-K_s$ diagram in the top, the dotted (blue) lines are the approximate completeness and detection limits of the combined DENIS-2MASS cross-correlation. The solid (black) line is the criterion for selecting cluster stars and brown dwarfs without known features of youth in σ Orionis used by Caballero (2008c). The dashed (black) line is the criterion shifted bluewards by 0.25 mag. The reddest sources in the $J-K_s$ vs. $i-J$ diagram in the bottom, with colours $J-K_s > 1.5 \text{ mag}$, are the galaxies UCM0536–0239 and 2E 1456 and the T Tauri star Mayrit 609206 (V505 Ori).

metric member candidate in Sherry et al. (2004), was spectroscopically followed up by Sacco et al. (2007, 2008). They measured a radial velocity consistent with cluster membership, a faint H α (chromospheric) emission, and a peculiar underabundance of lithium. They derived nuclear and isochronal ages about 10 Ma older than expected for σ Orionis stars. Mayrit 605079 might belong to a differentiated young stellar population in the Orion Belt (Jeffries et al. 2006; Caballero 2007a; Maxted et al. 2008) or be instead an active field M-dwarf interloper with CN contamination around the Li I line (Caballero 2010).

2.5.2. Field stars

Caballero (2006) took high-resolution spectra of the two stars associated to the HRC-I sources Nos. 42 and 69, and found no trace of Li I in absorption (except for H α when it is in emission, the Li I line is the most obvious spectroscopic feature in young σ Orionis stars of the same magnitude as Nos. 42 and 69). The two of them were classified as non-cluster members by Caballero (2008c).

The star associated to the HRC-I source No. 51 was a photometric cluster member candidate in Sherry et al. (2004), but it has no lithium absorption, radial velocity, and H α emission consistent with membership in σ Orionis according to Sacco et al. (2008).

A fourth star, associated to the HRC-I source No. 31, was discovered and spectroscopically investigated by Wolk (1996). Its X-ray emission has been measured with *ROSAT* (Wolk 1996), *XMM-Newton* (Francis et al. 2006), and *Chandra* (Skinner et al. 2008). Given its location in the colour-magnitude diagram in Fig. 4, close to the confirmed field stars investigated by Caballero (2006) and its unclear spectroscopic information (see footnote to Table 1), we classify it as a “possible field star”.

2.5.3. Galaxies

There are two galaxies among the 90 HRC-I sources with 2MASS counterpart. One is the very bright X-ray galaxy 2E 1456 (No. 9), which is extended in optical and near-infrared images. Besides, it has blue colours in the optical and red ones in the near infrared (Caballero 2008c), an X-ray spectral energy distribution typical of an active galactic nucleus (López-Santiago & Caballero 2008), and irregular X-ray variability (Caballero et al. 2009). Bright X-ray galaxies towards the σ Orionis cluster are not uncommon (see also 2E 1448 in López-Santiago & Caballero 2008, which is out of the HRC-I field of view). The other cross-matched galaxy is UCM0536–0239 (No. 64). It is a Type 1 obscured quasi-stellar object at a spectroscopic redshift $z_{sp} = 0.2362 \pm 0.0005$ (Caballero et al. 2008 and references therein). The two galaxies have peculiar colours if compared to stars without thick discs (Fig. 4).

2.6. X-ray light curves

We built 107 X-ray light curves to look for flares and rotational modulation in young stars. For each X-ray source, we integrated the numbers of HRC-I counts in two circular areas of the same radius, one centred on the source itself and the other one in a region free of X-ray sources for subtracting the background level. The integration radii varied between 7 and 30 arcsec depending on the offaxis distance (i.e., the size of the point spread function). The bin size was fixed to 1200 s. We discarded the first 5 ks of each light curve because they were affected by a relatively high background (this effect was only appreciable in the faintest sources; Fig. 5).

Next, we followed the same Poisson- χ^2 analysis as in Caballero et al. (2009) on the 107 X-ray light curves to identify variable sources (Fig. 6). This analysis provides similar re-

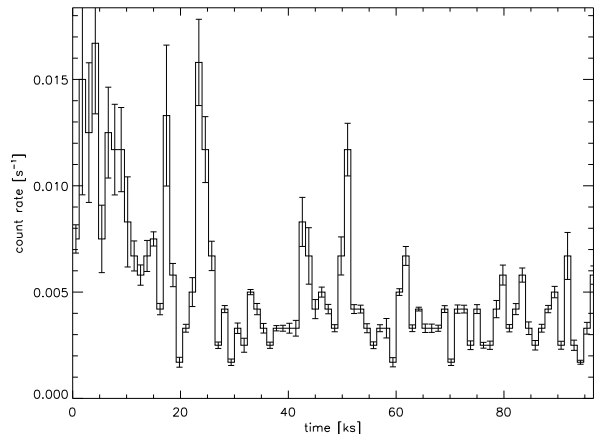


Fig. 5. A median HRC-I background light curve. Note the high, decreasing, background level during the beginning of the observation.

Table 3. Sources with a probability of X-ray variability in the HRC-I data larger than $p_{\text{var}} = 99.5\%$.

No.	Name	\overline{CR} [ks ⁻¹]	χ^2	Variability type
4	Mayrit 348349	29.1	12.5	Flare decay
7	Mayrit 789281	54.9	24.8	Flare
8	Mayrit 863116 AB	55.6	26.3	Flare with structure
11	Mayrit 156353	13.0	3.6	Flare
13	Mayrit 180277	11.8	4.1	Flare
18	Mayrit 403090	11.0	4.5	Rot. modulation?
27	Mayrit 489165	8.0	3.2	Flare
28	Mayrit 489196	8.0	4.5	Rot. modulation?
30	Mayrit 397060	5.4	4.1	Flare

sults as applying Kolmogorov-Smirnov tests or carrying out a visual inspection of the light curves. We used the parameters $A = 76$, $B = 0.40 \text{ ks}^{-2}$, and $s = 2$ in the sigmoid relation between the number of events and the mean count rate, and the expression $\delta CR_i = 0.91287 CR_i^{1/2}$ in the relation between the individual count rates and their errors. In the case of the *Chandra* data, the above relations had much lower uncertainties than for the *ROSAT* data in Caballero et al. (2009).

Nine X-ray sources had probabilities of variability larger than a conservative value of $p_{\text{var}} = 99.5\%$ (Table 3 and Fig. 7). The nine of them are σ Orionis stars with signposts of youth. Three stars (Nos. 7, 8, and 13) displayed apparent flares with peak-to-quiescence ratios of about six and durations longer than 20 ks. Besides, we detected in star No. 4 the long-lasting decay of a flare with an expected peak-to-quiescence ratio larger than six. Other three stars (Nos. 11, 27, 30) also displayed flares during the observations. On the contrary to the other two stars, the flare observed in the star No. 30 was relatively faint and short (it showed a “spike” flare following the nomenclature by Wolk et al. 2005).

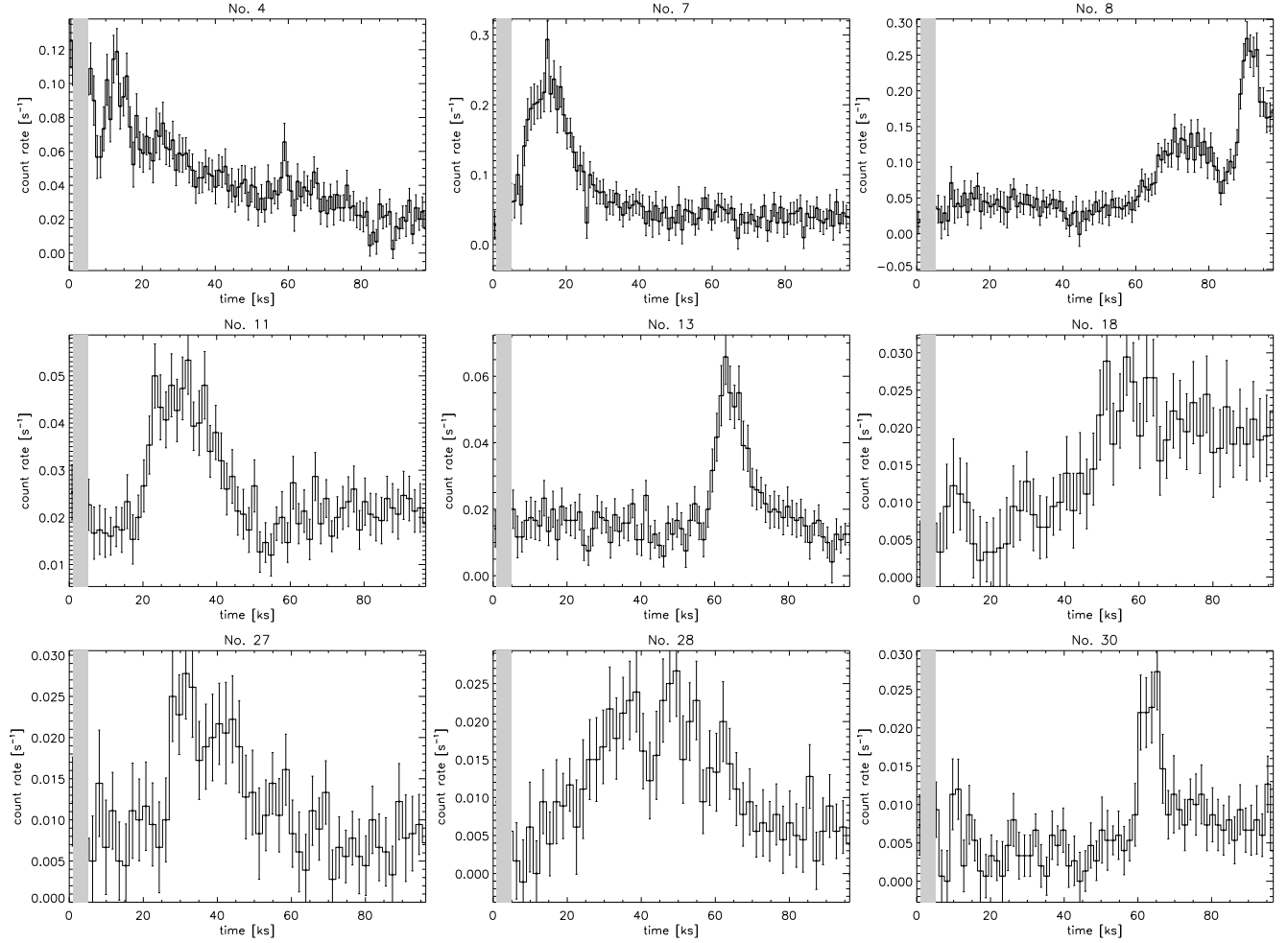


Fig. 7. HRC-I/*Chandra* light curves of the nine X-ray variable stars in Table 3. The grey areas between 1 and 5 ks indicate portions of all the light curves affected by high background.

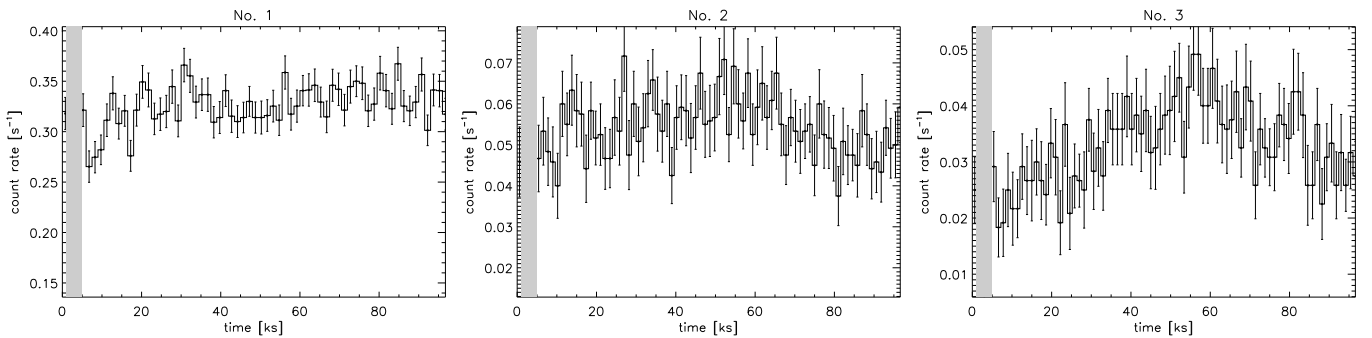


Fig. 8. Same as Fig. 7, but for three brightest X-ray stars: Mayrit AB (σ Ori AB, No. 1), Mayrit 114305 AB ([W96] 4771–1147 AB, No. 2), and Mayrit 42062 AB (σ Ori E, No. 3).

The two remaining stars, Nos. 18 and 28, showed variations not clearly attributable to “usual” flares. The light curve of the source No. 28 is similar to that observed for σ Ori E, a star with rotationally-modulated X-ray emission (see below). The case of the source No. 18 is more complex. The count-rate enhancement suffered at about 40 ks from the beginning of the observation could be related to a persistent flare, although occultation of part of the corona by a companion or of an active

region by stellar rotation should not be discarded. Nevertheless, since HRC-I does not provide spectral energy information, we could not perform an analysis of the time-resolved spectra to corroborate the hypothesis of rotational modulation in the light curves of the stars Nos. 18 and 28.

To date, there have been few incontestable cases of X-ray rotational modulation in the σ Orionis cluster (e.g., Franciosini et al. 2006). The most documented case is that of the bright

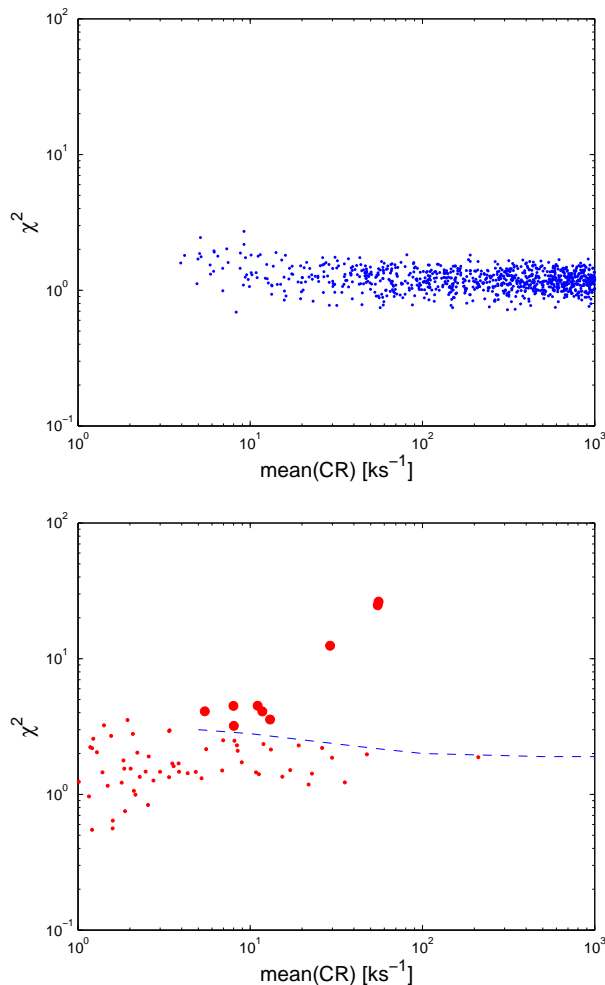


Fig. 6. *Top:* χ^2 as a function of the mean count rate (χ_j^2 vs. \overline{CR}_j diagram) for 10^3 of the 10^5 X-ray simulated series. *Bottom:* same as top window, but for the 107 X-ray real series. X-ray sources above the dashed line have probabilities larger than 99.5 % of being actual variables. Light curves with mean count rates lower than 5 ks^{-1} were not used in the statistical analysis. Compare this figure with the Fig. 6 in Caballero et al. (2009).

B2Vpe star σ Ori E (Mayrit 42062 AB, No. 3), which was found to have an X-ray emission modulated with a period consistent with the stellar rotation, $P \sim 1.19 \text{ d}$ ($P \sim 103 \text{ ks}$; Townsend et al. 2010 and references therein), by Skinner et al. (2008). Our Poisson- χ^2 analysis gave σ Ori E a low probability of variability. However, Caballero et al. (2009) noticed that the methodology was sensitive to flaring activity, but not to low-amplitude modulation. We visually inspected the X-ray light curve of σ Ori E and detected a modulation with a sinusoidal-like variation of the HRC-I count rate between 20 and 50 ks^{-1} and an estimated period slightly longer than the duration of the observations ($>97.6 \text{ ks}$), which is also consistent with the rotational period. On the contrary to Groote & Schmitt (2004), Sanz-Forcada et al. (2004), and Caballero et al. (2009), who reported strong X-ray flares in the light curves of σ Ori E, we found any (the flares are originated in its low-mass companion; Caballero et al. 2009). The light curve of σ Ori E is displayed in

the right panel of Fig. 8 in comparison with the two brightest X-ray sources in our HRC-I observations. The supposed stable light curve of σ Ori AB (Mayrit AB, No. 1), whose X-ray emission is likely originated in a strong wind (in particular for σ Ori AB: Sanz-Forcada et al. 2004; Skinner et al. 2008 – in general for OB stars: Lucy & White 1980; Owocki & Cohen 1999; Kudritzki & Puls 2000 Güdel & Nazé 2009), had a χ^2 value slightly below the limit p_{var} that we adopted for variability, just as it occurred during the ACIS-S observations by Skinner et al. (2008). The light curve of the classical T Tauri star Mayrit 114305 AB ([W96] 4771–1147 AB, No. 2) had a lower χ^2 value of about 1.2, but showed a hint of rotational modulation.

2.7. Beyond the completeness

We performed a new search of X-ray sources in our HRC-I data by imposing a less-restrictive identification criterion. In Section 2.3, we established only one spurious X-ray source among the 107 (actually 109) detections. In this case, we eased the identification of very faint sources close to the noise limit by setting to ten the maximum of spurious X-ray sources with PWDetect. The corresponding background level translated into a final threshold of significance of detection $S_{\text{min}} = 4.6\sigma$ (it was $S_{\text{min}} = 5.1\sigma$ for a maximum of one spurious X-ray source). The less-restrictive choice resulted in the detection of 142 sources (i.e., we gained about 24 new reliable sources by accepting nine extra spurious detections). However, the gain was not considerable because of the large contamination by extragalactic sources at low X-ray count rates.

Of the 33 newly identified sources, we list five in Table 4. Four of them were identified in the X-ray observations by Franciosini et al. (2006). One of the four sources was also identified by Skinner et al. (2008), which supports our X-ray detections beyond the completeness. There is optical/near-infrared counterpart for all HRC-I sources in Table 4 except for [FPS2006] NX 120 ([SSC2008] 40), which is probably a galaxy (Franciosini et al. 2006)⁹. The four cross-matched X-ray sources are σ Orionis cluster members and candidates with faint X-ray emission (Caballero 2008c). Of them, only Mayrit 441103 has no known feature of youth. We followed the criterion in López-Santiago & Caballero (2008) to discard the remaining 29 X-ray sources without 2MASS counterpart (including [SSC2008] 40) as stellar/substellar candidates, and classified them as objects of extragalactic nature.

3. Discussion

3.1. Short-term X-ray variability: HRC-I light curves

The nine X-ray variable sources in Table 3 are young stars in the σ Orionis cluster. This makes a minimum frequency of X-ray variability of 11 % (9/84; it increases to 12 % if we take into account σ Ori E). The reader should compare this value with

⁹ At less than 6 arcsec from [FPS2006] NX 120 lie 2MASS J05385930–0235282, a fore- or background source based on *iJHK_s* colours, and [BZR99] S Ori 72, a young L/T-transition cluster member candidate or active galactic nucleus (Bihain et al. 2009).

Table 4. Previously-known sources in the 10-spurious search and not in Table C.1.

Name	α (J2000)	δ (J2000)	$\Delta\alpha, \Delta\delta$ [arcsec]	S (σ)	Offaxis [arcmin]	CR [ks ⁻¹]	NX (Fr06)	CXO (Sk08)	Remarks
Mayrit 734047	05 39 20.44	-02 27 36.8	5.54	4.92	12.0	2.1 \pm 0.6	159	...	Li I, H α
Mayrit 468096	05 39 15.83	-02 36 50.7	2.09	4.83	7.60	0.6 \pm 0.2	151	...	Li I, Class II
Mayrit 441103	05 39 13.47	-02 37 39.1	1.58	4.62	7.13	0.42 \pm 0.14	148
[FPS2006] NX 120	05 38 59.51	-02 35 28.6	0.83	4.67	3.47	0.23 \pm 0.08	120	40	Galaxy
Mayrit 270181	05 38 44.49	-02 40 30.5	0.90	4.71	4.60	0.22 \pm 0.09	Li I, low g

the ones of 36 and 39 % reported by Franciosini et al. (2006) and Caballero et al. (2009), respectively, in the same cluster, but using different sampling and datasets (in practice, 43 ks of continuous observations with *XMM-Newton* –Franciosini et al. 2006– and one *ROSAT* visit per day during 34 days –Caballero et al. 2009–). Although Skinner et al. (2008) did not provide a frequency, we estimated a rough value at 25 % from their data (see below). We ascribed the low frequency derived by us to our conservative variability criterion, rather than to the different completeness depths of the surveys. Our value of 11 % is a lower limit to the X-ray frequency because there are probable variable young stars that did not pass our filter. For example, stars Nos. 16 (Mayrit 97212) and 17 (Mayrit 157155), which were not listed in Table 3, displayed hints of rotational modulation and flaring activity, respectively, after a visual inspection.

We also compared our derived flare rate with other measurements in the literature. With seven flares detected during our observation among 84 young stars and candidates, we derived 1/1180 flares per star per kilosecond. This value decreased to less than about 1/1070 when we discarded the early-type (OB) cluster stars (Section 3.3.1). Both corrected and uncorrected values are consistent with previous determinations of flare rates, although we did not consider the completeness for flare detection. For example, with different instruments, sensitivities, flare definitions and energies, data biases, extragalactic contaminations, and stellar spectral-type intervals, Wolk et al. (2005), Albacete-Colombo et al. (2007), and Stelzer et al. (2007) reported flare rates of 1/1150, 1/610, and 1/1320 flares per star per kilosecond, respectively, in star-forming regions slightly younger than σ Orionis (Orion Nebula Cluster, Cyg OB2, and Taurus; $\tau \sim 1\text{--}2$ Ma).

Several stars in Table 3 have been previously reported to display X-ray variability. By applying Kolmogorov-Smirnov tests on the unbinned photon arrival times, Franciosini et al. (2006) found that roughly a half of the (weak-line and classical) T Tauri stars in σ Orionis were variable at the 99 % confidence level. Eight cluster members with signposts of youth and two candidate members showed clear flares during their *XMM-Newton* observations. Of them, we were able to detect the X-ray emission in the HRC-I image of five stars, of which only one displayed variability during our observations (No. 28, Mayrit 489196, [FPS2006] NX 61), but of rotational-modulation type. However, the two X-ray light curves obtained with *XMM-Newton* and *Chandra* resemble each other, so we

may face the same variability type (e.g., a low-amplitude, long-lasting flaring activity). Franciosini et al. (2006) also reported five young stars showing significant variability not clearly attributable to flares. We detected the five of them and found that one, No. 11 (Mayrit 156353, [FPS2006] NX 76), displayed a flare during our observations. In contrast, during the entire *XMM-Newton* observations, the star showed a steady decay by a factor of ~ 2 , which we attribute to the decay of a long-lasting flare. The frequencies of X-ray rotational modulation reported by us and Franciosini et al. (2006) are consistent with the approximate interval 1–3 %.

The list of ten variables in Skinner et al. (2008) included Mayrit 42062 AB (σ Ori E; see above), the unseen galaxy associated to No. 24 (a slow low-amplitude variable X-ray with unusual hardness and without optical/near-infrared counterpart), and some young stars with slow decline (No. 5, Mayrit 203039) or increase (No. 25, Mayrit 3020 AB) in count rate. Besides, X-ray flares were visible in Mayrit 105249 (No. 12; variable in Franciosini et al. 2006) and, possibly, Mayrit 92149 AB (No. 29). If we do not take into account σ Ori E, there are no stars in common in the lists of variable X-ray sources in Skinner et al. (2008) and our work.

Besides, two of the five most variable stars in the study by Caballero et al. (2009; Section A.2) appear also in Table 3. They are Mayrit 863116 AB (No. 8) and Mayrit 156353 (No. 11). Interestingly, the HRC-I light curve of the bright star Mayrit 863116 AB showed a flare with structure. The double hump may be originated in a series of two flares of different shape or in only one flare that was occulted by stellar rotation, a companion, or a disc (Mayrit 863116 AB seems to be a spectroscopic binary with a warm circumstellar disc; Caballero et al. 2009).

There are only a few stars that have been repeatedly found to display the same X-ray variability type, such as the bright early-type σ Ori E and T Tauri Mayrit 863116 AB stars. To sum up, some young X-ray stars that displayed variability at other epochs did not do it during our observations, and vice versa. This result was expected from the relatively low flare rate measured above of one flare per star every one or two weeks. As a result, the variability frequencies given above depend on several factors including the sensitivity, length, and energy band-pass of the observation and can only be taken as lower limits.

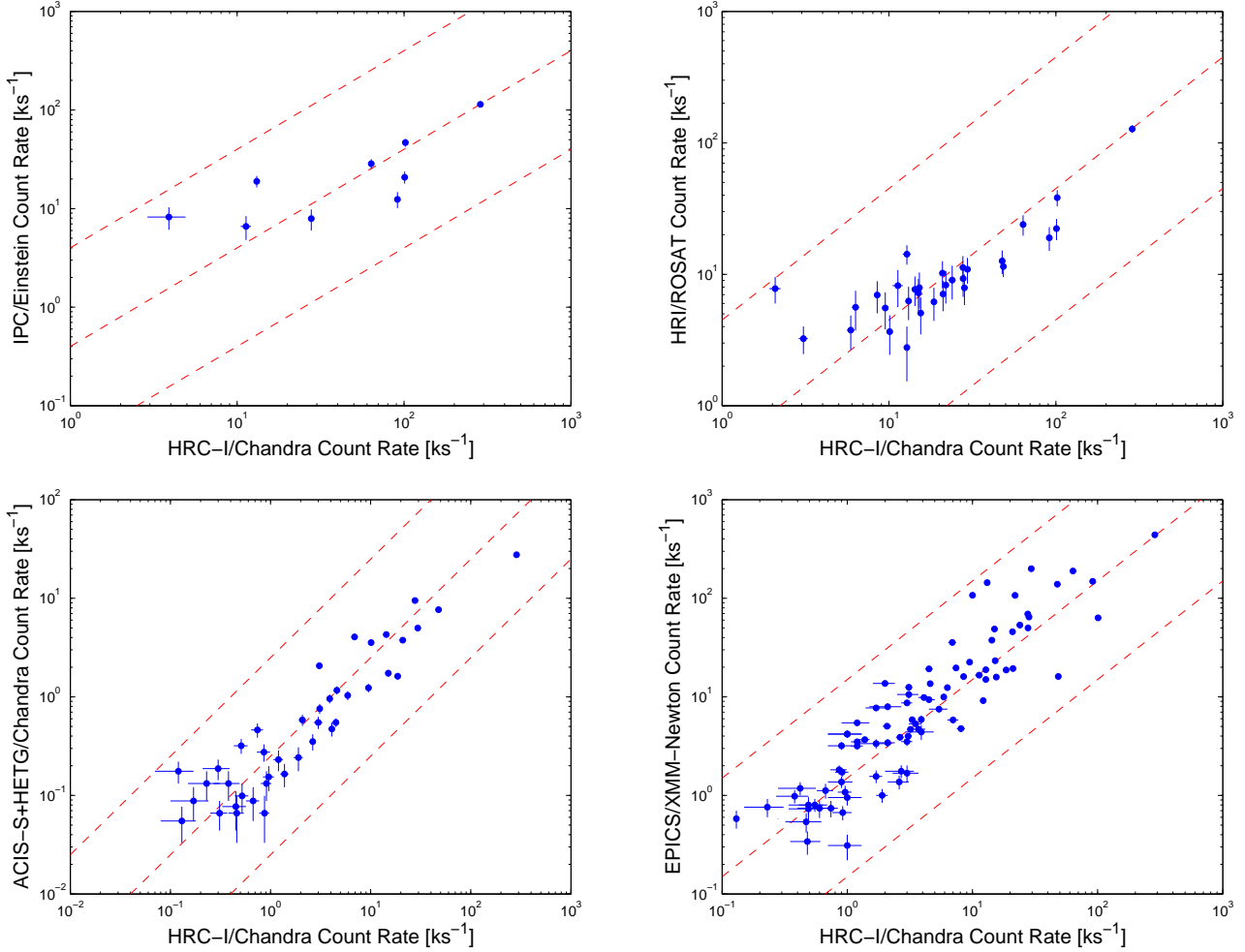


Fig. 9. Count rates of IPC/*Einstein* (top left), HRI/*ROSAT* (top right), ACIS-S+HETG/*Chandra* (bottom left), and EPIC/*XMM-Newton* (bottom right) as a function of count rates of HRC-I/*Chandra*. The dashed lines indicate IPC–, HRI–, ACIS-S+HETG–, and EPIC–HRC-I count-rate ratios of 4.00, 0.40, and 0.04, 4.50, 0.45, and 0.045, 2.50, 0.25, and 0.025, and 15.0, 1.50, and 0.15 from top to bottom, respectively. The OB-type binary star σ Ori AB has *not* been used as a reference in the ACIS-S+HETG–HRC-I comparison.

3.2. Long-term X-ray variability: comparison to previous X-ray surveys in σ Orionis

All the large space missions able to observe low- to mid-energy X-rays, i.e. *Einstein Observatory* (HEAO-2), *ROSAT* (Röntgensatellit), *XMM-Newton*, and *Chandra*, have observed the σ Orionis region in detail (Section A). Besides, the Advanced Satellite for Cosmology and Astrophysics (ASCA) observed nearby areas close to the Horsehead Nebula and Alnitak (ζ Ori). In principle, the different pointing centres and exposure times of the observations, the singular apertures, fields of view, spatial resolutions and, specially, detector responses of the instrument/telescope systems (Table 5), and the “colours” and intrinsic variability of the X-ray sources avoid a direct comparison between previous results and ours. In spite of these differences, we expected to find a correlation between count rates measured by HRC-I and the other used instruments and to identify X-ray sources that deviate from the gen-

eral trends. See, e.g., the *Einstein-ROSAT* comparison in the Pleiades by Stauffer et al. (1994).

The “long-term variability” found in our comparison and summarised in Table 6 and Fig. 9 may actually be the result of observing an X-ray source with short- or mid-term variability (in scales of hours or a few days; e.g., flares) at two separated epochs. In particular, nine σ Orionis stars and one galaxy displayed quotients of the measured and average count-rate ratios larger than 4 or smaller than 1/4. Some of them showed variations of a factor 7 or more or were identified to vary in different comparisons:

- No. 3/Mayrit 42062 AB underwent flaring-like activity during the EPIC observations.
- No. 4/Mayrit 348349 showed an apparent flare decay during our HRC-I observations and other strong flare during the HRI/*ROSAT* ones.
- No. 16/Mayrit 97212 and No. 20/Mayrit 344337 AB showed significant variability not clearly attributable to flares during the EPIC observations.

Table 5. Energy bands, spatial resolutions, and field of view of some X-ray instruments onboard space missions^a.

Space mission	Instrument	Energy [keV]	Resolution [arcsec]	FoV [arcmin]
<i>Einstein</i>	HRI	0.2–3.0	4	25
	IPC	0.3–3.5	60	75
<i>ROSAT</i>	HRI	0.1–2.4	5	20 × 20
	PSPC	0.1–2.4	15	114
<i>Chandra</i>	HRC-I	0.08–10	0.4	31 × 31
	ACIS-S	0.2–10	1.2	16 × 16
<i>XMM-Newton</i>	PN	0.2–15	6	30
	MOS	0.2–12	6	30

^a See an exhaustive compilation of parameters of X-ray detectors at http://space.mit.edu/~jonathan/xray_detect.html.

Table 6. Long-term X-ray variable stars.

No.	Name	Variability factor ^b	Instrument
3	Mayrit 42062 AB	4.5	EPIC
4	Mayrit 348349	0.22	EPIC
16	Mayrit 97212	7.2	EPIC
20	Mayrit 344337 AB	7.3	EPIC
37	Mayrit 102101 AB	8.3	HRI
80	Mayrit 497054	4.6	EPIC
84 ^a	Mayrit 433123	0.21	EPIC
97	No. 97	5.9	ACIS-S
99	Mayrit 957055	5.2	IPC
...	Mayrit 631045 ^f	≥4.8	EPIC
...	Mayrit 662301 ^f	≥6.3	EPIC
...	Mayrit 841079 ^f	≥4.4	EPIC

^a See Section 3.3.2 for a discussion on the brown dwarf No. 84/Mayrit 433123.

^b Quotient of the measured count-rate ratio CR_1/CR_2 and the average count-rate ratio $(CR_1/CR_2)_0$, where 1 denotes the space-mission instrument listed in the last column and 2 denotes HRC-I/*Chandra*. The values of $(CR_1/CR_2)_0$ are 0.40 (IPC/*Einstein*), 0.45 (HRI/*ROSAT*), 0.25 (ACIS-S/*Chandra*), and 1.50 (EPIC/*XMM-Newton*).

- No. 37(Mayrit 102101 AB underwent a strong flare during HRI observations.
- The stars Mayrit 631045, Mayrit 662301, and Mayrit 841079, with designations NX 149, NX 7, and NX 174, respectively, in Franciosini et al. (2006; Section A.4) displayed flares and were bright enough during EPIC observations to be fitted to one-temperature models. Mayrit 841079 (V603 Ori) is the source of the Herbig-Haro object HH 445 (Reipurth et al. 1998; Andrews et al. 2004).

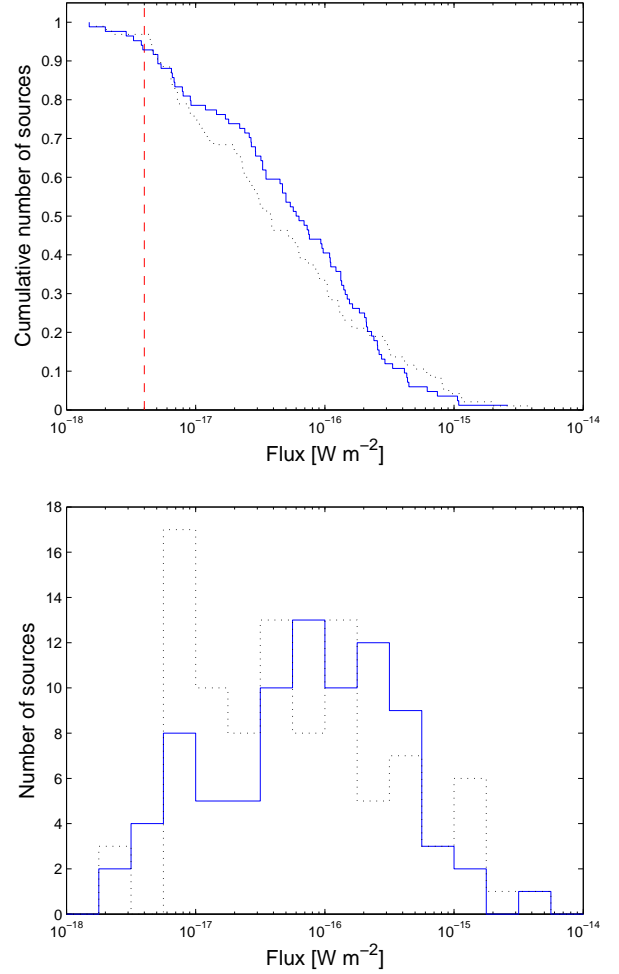


Fig. 10. *Top panel:* same as Fig. 2, but only for young stars, young star candidates, and possible young stars in σ Orionis (as classified in Table C.1). The dotted line indicates the relative cumulative number of Franciosini et al. (2006) EPIC X-ray sources as a function of apparent flux. Except for a $4\pi d^2$ factor, the two curves delineate the cumulative X-ray luminosity function of the cluster. *Bottom panel:* same as the top panel, but in an histogram.

3.3. The cluster X-ray luminosity function

The X-ray luminosity functions (XLFs) of young star clusters have been extensively studied during the last three decades. The *ROSAT* XLFs of the Pleiades, Hyades, or α Persei ($\tau \sim 90$ –600 Ma, $d \sim 45$ –190 pc – Stauffer et al. 1994; Stern et al. 1995; Randich et al. 1996) represented a cornerstone until the advent of *Chandra* and *XMM-Newton*. By taking advantage of the improved spatial resolution of these space missions currently under operation, clusters at longer heliocentric distances but with much younger ages than the three of them above have been studied in detail since, such as the Orion Nebula Cluster, IC 348, NGC 1333, NGC 2264, or M 17 ($\tau \sim 1$ –10 Ma, $d \sim 260$ –1600 pc – Feigelson et al. 2002; Preibisch & Zinnecker 2002; Getman et al. 2002; Flaccomio et al. 2006; Broos et al. 2007). In spite of the low number of X-ray emitters investi-

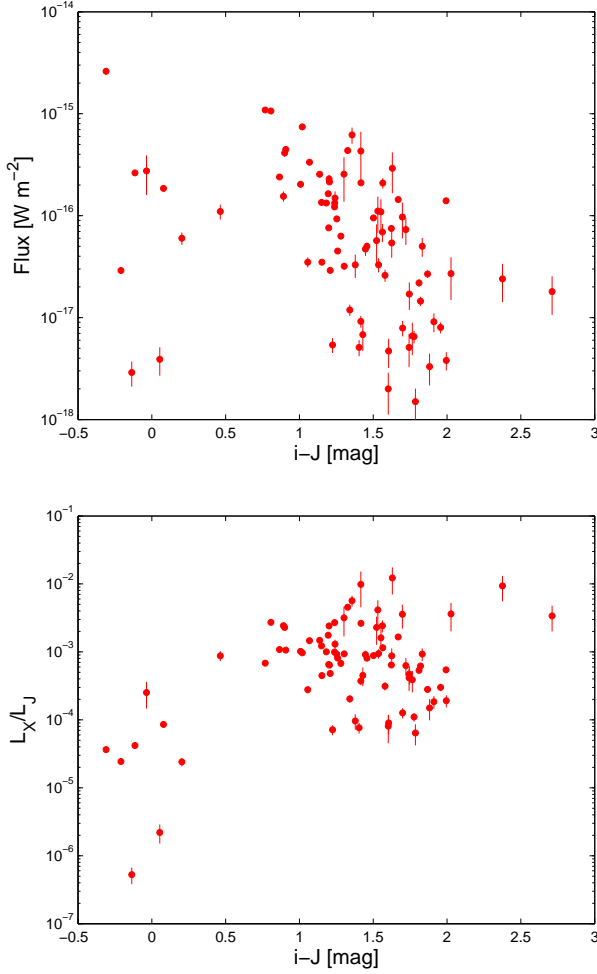


Fig. 11. X-ray flux (*top*) and X-ray-to-*J*-band luminosity ratio (*bottom*) as a function of the $i - J$ colour. Error bars account for the uncertainty in count rate and offaxis separation.

gated in σ Orionis with respect to the star-forming regions listed above, it has still a number of advantages, e.g., nearness, very low visual extinction, and wide knowledge of its stellar and substellar populations (Section 1).

Franciosini et al. (2006) already investigated the XLF of σ Orionis. We illustrate the classical approach with Fig. 10. The HRC-I median flux of all the cluster members and candidates, without attending to its spectral type, is $6.2 \cdot 10^{-17} \text{ W m}^{-2}$. We transformed back the X-ray luminosities tabulated by Franciosini et al. (2006) to fluxes (see below). For seven σ Orionis stars detected by them but without luminosity determination, we used their EPIC count rates and count-rate-to-flux conversion factor. Except for slight differences that can be ascribed to the different spectral sensitivity of HRC-I and EPIC and method of flux estimation, the Franciosini et al. (2006) XLF and ours are quite similar.

Because of the long-lasting debate on the actual cluster distance and the absence of spectral-type determination for all the σ Orionis members and candidates, we preferred instead the diagrams in Fig. 11 for our XLF discussion. Both the apparent X-ray flux (top panel) and the X-ray-to-*J*-band luminosity ra-

tio (bottom panel) are independent of the actual distance, while there are accurate $i - J$ measurements for all the X-ray stars and brown dwarfs in σ Orionis, mostly taken from Caballero (2008c). The optical/near-infrared colour $i - J$ is a suitable indicator of effective temperature (i.e., of spectral type). The use of other colours involving bluer optical and redder near-infrared bands (e.g., $V - J$, $i - K_s$) is currently impractical because of no data availability (all the faintest cluster members lack *B*-, *V*-, and *R*-band measurements) or flux excesses at wavelengths longer than $1.2 \mu\text{m}$ in cluster members with circum(sub)stellar material. The X-ray-to-*J*-band luminosity ratio, L_X/L_J , is defined by:

$$\frac{L_X}{L_J} = \frac{4\pi d^2 \mathcal{F}_X}{4\pi d^2 \mathcal{F}_J}, \quad (1)$$

where $\mathcal{F} \equiv \lambda F_\lambda$ is the apparent flux, in watts per square meter, and the apparent *J*-band flux \mathcal{F}_J is approximately proportional to the apparent bolometric flux \mathcal{F}_{bol} . The spectral energy distribution of late-K- and M-type stars peak at the *J* band, which is besides the band least affected by photometric variability and presence of discs. The L_X/L_J ratio is thus a proxy for L_X/L_{bol} .

Diagrams showing X-ray-to-*J*-band luminosity ratio as a function of colour/effective temperature/spectral type, as in the bottom panel in Fig. 11, have been shown by, e.g., Micela et al. (1999), Reid (2003), and Daemgen et al. (2007). In our diagram, three different regions can be separated: massive early-type stars (mostly OB), intermediate- and low-mass stars (GKM), and brown dwarfs (with spectral types later than about M5.5 in σ Orionis).

3.3.1. Early-type stars

With HRC-I/*Chandra*, we identified eight σ Orionis stars with spectral types earlier than F0, listed in Table 7. The list includes three stars in the eponymous σ Ori Trapezium-like system with spectral types B2 or earlier. In Fig. 11, the eight of them have colours $i - J \lesssim 0.2 \text{ mag}$ and display a wide range of L_X/L_J ratios.

The spectral types in Table 7 were borrowed from the bright-star compilation in Caballero (2007a), except for the secondaries in the binary systems Nos. 3 and 10 (a colon, “:”, after a spectral type denotes uncertainty; the letters “p” and “e” indicate peculiarity and emission, respectively). We estimated a K–M: spectral type for Mayrit 42062 B, the companion at $\rho \approx 0.33 \text{ arcsec}$ to σ Ori E, based on its approximate K_s magnitude as evaluated by Bouy et al. (2009). The estimation of the late B-early A spectral type for Mayrit 306125 B, the companion at $\rho \approx 0.47 \text{ arcsec}$ to Mayrit 306125 A (HD 37525), was taken from Caballero et al. (2009). The brightest star in the cluster, No. 1/ σ Ori AB + “F”, seems to be actually a close triple systems of OB stars (Frost & Adams 1904; Bolton 1974; Caballero 2008a; S. Simón-Díaz et al., in prep.). Only two stars, No. 53/Mayrit 524060 and No. 88/Mayrit 960106, are not known to form part of a multiple system.

Of the eight early-type stars, three (Nos. 1, 3, and 10) were bright enough in X-rays for HRI/*ROSAT* to be analysed by Caballero et al. (2009). Other three stars (Nos. 34, 53, and 74) were detected with EPIC/*XMM-Newton* by Franciosini et al.

Table 7. Early-type stars in σ Orionis detected with HRC-I/*Chandra*.

No.	Name	Alternative name	Spectral type
1	Mayrit AB	σ Ori AB + “F”	O9.5V + B0.5V + ?
3	Mayrit 42062 AB	σ Ori E	B2Vpe + K–M:
10	Mayrit 306125 AB	HD 37525 AB	B5Vp + B–A:
34	Mayrit 189303	HD 294272 B	B8V
53	Mayrit 524060	HD 37564	A8V:
70	Mayrit 13084	σ Ori D	B2V
74	Mayrit 182305	HD 294272 A	B9.5III
88	Mayrit 960106	V1147 Ori	B9IIIp

(2006). In practice, they could not resolve the X-ray emission coming from the system HD 294272 (No. 34/Mayrit 189303 and No. 74/Mayrit 182303). The pair was first resolved in X-rays by Caballero (2007a) using our HRC-I/*Chandra* dataset. Of the other two stars, No. 88/Mayrit 960106 was detected with PSPC/*ROSAT* by White et al. (2000) but escaped other X-ray surveys. The presence of the last star, No. 70/Mayrit 13084 (σ Ori D), in the current HRC-I data was already noticed by Sanz-Forcada et al. (2004), Caballero (2007b), and Skinner et al. (2008), but it has never been analysed. The B2V star was not detected either with HRI-PSPC/*ROSAT*, EPIC/*XMM-Newton*, or ACIS-S/*Chandra*.

The early-type stars with the lowest L_X/L_J ratios were No. 70/Mayrit 13084 and No. 74/Mayrit 182303, which justified previous undetections, while the star with the highest L_X/L_J ratio was No. 88/Mayrit 960106. This is the B9-type giant V1147 Ori, an α^2 CVn-type variable with peculiar silicon abundance (Joncas & Borra 1981; North 1984; Catalano & Renson 1998). Its undetection in previous surveys with HRI/*ROSAT*, EPIC/*XMM-Newton*, and ACIS-S/*Chandra* may reside simply in its location in σ Orionis, at about 16 arcmin to the east of the cluster centre.

Only a few σ Orionis stars more massive than $2.5 M_\odot$ (Caballero 2007a) have not been detected with HRC-I/*Chandra*. They are Mayrit 208324 (HD 294271, B5V), Mayrit 1116300¹⁰ (HD 37333, A1Va – but see Naylor 2009), and Mayrit 11238 (σ Ori C, A2V). The star HD 37699, a young B5V star with an envelope at 25.8 arcmin to the cluster centre, seems to be associated to the stellar population near the Horsehead Nebula (Caballero & Dinis 2008).

In summary, with HRC-I/*Chandra* we detected all the σ Orionis stars more massive than $5 M_\odot$ (σ Ori AB, D, E) and roughly two thirds of the stars with masses in the interval 2.5 to $5 M_\odot$. Stars in multiple systems or with spectral peculiarities tend to be among the stars with detected X-ray emission.

3.3.2. Brown dwarfs

Two red cluster members with high L_X/L_J ratios stand out in the upper right corner of the bottom panel in Fig. 11, with colours $i - J \sim 2.4\text{--}2.7$ mag. They are two of the only three X-ray brown dwarfs detected in σ Orionis with EPIC/*XMM-Newton* by Franciosini et al. (2006): No. 84/Mayrit 433123 (S Ori 25 – Béjar et al. 1999; Muzerolle et al. 2003; Barrado y Navascués et al. 2003; Caballero et al. 2004, 2007) and No. 82/Mayrit 396273 (S Ori J053818.2–023539 – Béjar et al. 2004; Kenyon et al. 2005; Maxted et al. 2008). The third X-ray cluster brown dwarf, unidentified in our dataset, is Mayrit 487350 ([SE2004] 70, NX 67), which underwent a flare during the EPIC observations and is located at a relatively short projected physical separation to the planetary-mass object candidate S Ori 68 (Scholz & Eislöffel 2004; Caballero et al. 2006).

For Mayrit 396273, López-Santiago & Caballero (2008) imposed a maximum X-ray flux of $2.9 \times 10^{-17} \text{ W m}^{-2}$ from their EPIC/*XMM-Newton* observations to the west of σ Orionis, consistent with the flux reported here ($1.0 \pm 0.3 \times 10^{-17} \text{ W m}^{-2}$) and the flux estimated from the Franciosini et al. (2006) count rate ($\sim 0.6 \times 10^{-17} \text{ W m}^{-2}$). The brown dwarf may have a high X-ray quiescent level or underwent flares during both Franciosini et al. (2006) and our observations. Mayrit 396273 has the highest L_X/L_J ratio in σ Orionis after the two young star candidates No. 94/Mayrit 887313 and No. 98/Mayrit 1178039 (which are located at large offaxis separations).

The other brown dwarf, Mayrit 433123, is a photometric variable, emission-line, accreting, substellar object of only about $0.058 M_\odot$, well below the hydrogen burning mass limit (Caballero et al. 2007). From the long-term X-ray variability analysis in Section 3.2, Mayrit 433123 was about five times brighter at the HRC-I/*Chandra* epoch than at the EPIC/*XMM-Newton* one, which indicates that the brown dwarf could flare during our observations.

Unfortunately, we could not perform a spectral analysis of the two substellar objects and the low statistics prevented us to achieve conclusions on the origin of the X-ray emission from their light curves. One of the scenarios that could explain the X-ray emission in brown dwarfs is accretion from a circumsubstellar disc, since the high electrical resistivities in the neutral atmospheres of ultracool dwarfs are expected to prevent significant dynamo action (Mohanty et al. 2002; Stelzer et al. 2010). In fact, Mayrit 433123, with M6.5 spectral type and $p\text{EW}(H\alpha) \approx -44 \text{ \AA}$, satisfies the empirical criterion to classify accreting T Tauri stars and substellar analogues using low-resolution optical spectroscopy of Barrado y Navascués & Martín (2003). Besides, it seems to be rotationally locked to an imperceptible disc inclined $i \approx 46$ deg with respect to us (Caballero et al. 2004, 2007; Luhman et al. 2008). However, if a brown dwarf is young enough, it could still retain a (non self-sustained) primordial field. Furthermore, Stelzer et al. (2006) found that accreting brown dwarfs have lower X-ray luminosity than non-accreting ones and suggested that substellar activity is subject to the same mechanisms that suppress X-ray emission in pre-main-sequence stars during the T Tauri phase. The object statistics (two or three X-ray brown dwarfs) is still too poor to

¹⁰ López-Santiago & Caballero (2008) provided a restrictive upper limit of the EPIC/*XMM-Newton* apparent flux of Mayrit 1116300.

Table 8. Intermediate- and low-mass X-ray stars in σ Orionis with colours $J - K_s > 1.15$ mag^a.

No.	Name	Alternative name	$J - K_s$ [mag]	Sp. type	pEW(Li I) [mÅ]	pEW(H α) [Å]	SED class	Phot. variable
29	Mayrit 92149 AB	[W96] rJ053847–0237	1.24 \pm 0.06	M1.0:	481 \pm 8	–20.9 \pm 1.2	II	no
36	Mayrit 203283	[W96] rJ053831–0235	1.16 \pm 0.04	M0.0:	479 \pm 6	–10.2 \pm 0.9	II	no
45	Mayrit 609206	V505 Ori	2.01 \pm 0.04	K7.0	431 \pm 11	–25.1 \pm 0.7	II	yes
61	Mayrit 30241	[HHM2007] 687	1.28 \pm 0.05	II	no
72	Mayrit 521199	TX Ori	1.46 \pm 0.04	K4	...	–16.6	II	yes
75	Mayrit 622103	BG Ori	1.30 \pm 0.04	M0.5:	480 \pm 7	–40 \pm 3	II	yes
79	Mayrit 203260	Haro 5–11	1.19 \pm 0.04	M2.0:	342 \pm 2	–198 \pm 12	II	no
80	Mayrit 497054	V509 Ori	1.26 \pm 0.03	M0.5:	263 \pm 4	–25.8 \pm 0.8	II	yes

^a Spectral types and Li I and H α pseudo-equivalent widths are from Zapatero Osorio et al. (2002) and Sacco et al. (2008). The colon after the spectral type denotes a estimation based on photometry.

conclude whether X-rays from brown dwarfs originate via the same processes as from low-mass stars.

Using the same HRC-I/*Chandra* dataset, but with a coarse identification process, Caballero (2007b) listed two additional faint X-ray sources that were not identified by us, even during the 10-spurious search (Section 2.7). They could be related to the young very low-mass star Mayrit 50279 (Sacco et al. 2008) and the X-ray source [FPS2006] NX 77. Caballero (2007b) associated the latter to an infrared source with $J \sim 19.0$ mag and $J - K_s \sim 1.8$ mag (tentatively called Mayrit 72345). If it belonged to σ Orionis, it would be an L-type, planetary-mass object with an estimated mass of $7 M_{\text{Jup}}$. Bouy et al. (2009) agreed with this classification. However, it would have an extraordinary luminosity ratio larger than $L_X/L_{\text{bol}} \sim 10^{-1}$ and, thus, we consider it instead an active background galaxy candidate with very red infrared colours.

3.3.3. Intermediate- and low-mass stars

There are a few remarkable X-ray stars among the remaining cluster members and candidates that are neither early-type stars nor young brown dwarfs. One of them is No. 63/Mayrit 591158 ([W96] 4771–0026), which has a relatively blue colour $i - K_s \approx 0.46$ mag and lies in the L_X/L_J vs. $i - J$ diagram halfway between OB and active KM σ Orionis stars. Mayrit 591158 has cosmic lithium abundance, an effective temperature of about 6000 K, a high rotational velocity of $v \sin i = 60 \pm 5 \text{ km s}^{-1}$, a partially-filled H α absorption line, and [S II] and [N II] lines in emission (Caballero 2006; González-Hernández et al. 2008). This star is significantly warmer than the other six X-ray stars in the diagram with colours $0.5 \text{ mag} \lesssim i - J \lesssim 1.0 \text{ mag}$, all of which have strong lithium absorption lines and spectral type (or effective temperature) determinations between late-G–K0 and K7. As a result, Mayrit 591158 is the only X-ray emitter in σ Orionis with a spectral type between F and mid-G¹¹. This fact

is probably associated to the high reported rotational velocity, which may favour an enhancement of the magnetic activity.

Other remarkable X-ray source is the young low-mass star candidate No. 103/Mayrit 578123 ([FPS2006] NX 153), which is the third faintest X-ray source in our sample and has a high L_X/L_J ratio. We estimated a mass of about $0.08\text{--}0.09 M_\odot$ from its J -band magnitude as in Caballero et al. (2007). There is no spectroscopy available of Mayrit 578123 to confirm its membership in σ Orionis.

It has been widely discussed in the literature whether classical (accreting) T Tauri stars have a lower frequency and intensity of X-ray emission than weak-line (non-accreting) T Tauri stars (e.g., Feigelson et al. 1993; Neuhäuser et al. 1995; Preibisch & Zinnecker 2002; Telleschi et al. 2007 – see also Stelzer et al. 2006 for a discussion on X-ray emission from T Tauri-like brown dwarfs). In the σ Orionis cluster, Franciosini et al. (2006), Caballero (2007b), and López-Santiago & Caballero (2008) confirmed the real deficiency in classical T Tauri stars in the XLF. Some hypothesis have been presented to explain this deficiency, such as cooling of active regions by accretion or absorption of X-rays by dust in a circumstellar disc. In the second picture, the geometry of the star-disc system with respect to us plays a crucial rôle (i.e., edge-on discs occult the central object while front-on ones do not). Since the inclination angles of circumstellar discs are randomly distributed, we expect no relation between the strength of both the X-ray emission and near-infrared flux excess.

Following this discussion, we investigated the reddest KM-type X-ray stars in σ Orionis, which we expected to be classical T Tauri stars with discs. The eight X-ray stars with colours $J - K_s > 1.15$ mag listed in Table 8 have spectral energy distributions (from the optical to $8.0\text{--}24 \mu\text{m}$) typical of discs harbours according to Hernández et al. (2007). Except for No. 61/Mayrit 30241, which misses spectroscopy, all the stars satisfy the H α -accretion criterion of Barrado y Navascués & Martín (2003). Of them, only two stars, No. 72/Mayrit 521199 (TX Ori) and, specially, No. 45/Mayrit 609206 (V505 Ori, with $J - K_s = 2.01 \pm 0.04$ mag) have colours redder than 1.4 mag, while in σ Orionis there are about a dozen KM-type stars redder than this value (Caballero 2008c). For example, none of

¹¹ Furthermore, Mayrit 591158 and Mayrit 524060 (A8V:) are the only X-ray emitters in σ Orionis with spectral types between early-A and mid-G.

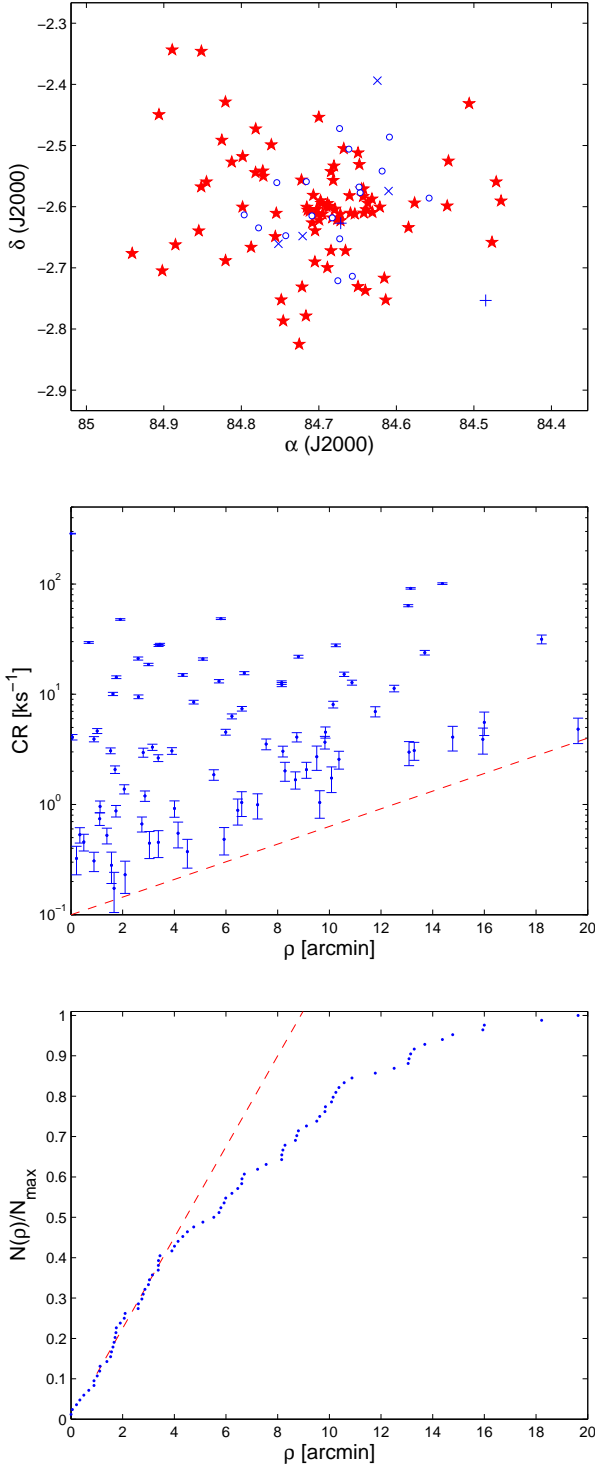


Fig. 12. *Top panel:* spatial location diagram. The different symbols represent: cluster star and brown dwarf members and candidates (–red– filled stars), field stars (–blue– crosses), galaxies with optical/near-infrared counterpart (–blue– pluses), and galaxies without counterpart (–blue– open circles). Size is 40×40 arcmin², with centre on σ Ori AB. *Middle panel:* count rate of σ Orionis stars as a function of the angular separation to the cluster centre. The dashed line sketches the approximate lower limit for detection of the HRC-I/*Chandra* observations. *Bottom panel:* relative cumulative number of X-ray σ Orionis star and brown dwarf members and candidates as a function of angular separation to the cluster centre, ρ . The dashed line indicates the expected values if the X-ray stars followed a volume-density law proportional to ρ^{-2} .

the stellar sources of the four Herbig-Haro objects in σ Orionis (Reipurth et al. 1998), which also have very red $J - K_s$ colours, were detected with HRC-I (but the source of HH 445 was detected by Franciosi et al. 2006 – Section A.4). Likewise, only six of the about thirty KM-type σ Orionis stars redder than $J - K_s = 1.2$ mag were detected with HRC-I. A detailed analysis of the frequency of X-ray emitters as a function of mass, disc presence, and degree of accretion is to be done, but the values above hint at a lower frequency and intensity of X-ray emission of classical (accreting) T Tauri stars in σ Orionis than weak-line (non-accreting) T Tauri stars.

3.4. Spatial distribution of X-ray sources

As a final analysis of the HRC-I data, we investigated the spatial distribution of X-ray stars in σ Orionis. From the top panel in Fig. 12, the cluster stars are concentrated towards the centre, defined by the eponymous σ Ori AB system, which coincides with the centre of the field of view with a small error of 13 arcsec (Section 2.1). The apparent concentration of galaxies without optical/near-infrared counterpart and field stars in the innermost 10 arcmin is due to the combined effect of their faintness and the decreasing sensitivity of the HRC-I detector at large offaxis separations. Only relatively bright X-ray fore- and background sources, such as the field star No. 69/[W96] rJ053829–0223 or, specially, the galaxy 2E 1456, could be detected at more than 10 arcmin to the pointing centre. The middle panel in Fig. 12 illustrates the effect of the degradation of the sensitivity towards the HRC-I borders: while roughly all the X-ray sources with count rates $CR > 0.1 \text{ ks}^{-1}$ were detected in the central area, the lower limit for detection increased up to about 1 ks^{-1} at 10 arcmin and about 4 ks^{-1} at 20 arcmin.

According to Caballero (2008a), the radial distribution of σ Orionis stars (without attending to their X-ray emission) follows a power law proportional to the angular separation to the cluster centre, ρ^{+1} , valid only for $\rho \lesssim 20$ arcmin. This distribution corresponds to a volume density proportional to ρ^{-2} , which is expected from the collapse of an isothermal spherical molecular cloud. From the bottom panel in Fig. 12, the X-ray stars in σ Orionis follow the power law ρ^{+1} only in the innermost 4 arcmin. Apart from the limited field of view of the detector, at large offaxis separations, the degradation of the sensitivity towards the HRC-I borders gets important and many X-ray σ Orionis stars were missed during the observations. We estimated that about 30 and more than 100 young stars and brown dwarfs were missed in the 4–10 and 10–20 arcmin annuli, respectively. The sensitivity degradation must be taken into account when frequencies of X-ray emitters are computed.

4. Summary

We carried out a detailed analysis of the X-ray emission of young stars in the σ Orionis cluster ($\tau \sim 3$ Ma, $d \sim 385$ pc). We analysed public HRC-I/*Chandra* observations obtained in November 2002. The wide field of view, long exposure time of 97.6 ks, and the superb spatial resolution of HRC-I/*Chandra* allowed us to detect 107 X-ray sources, many of which had

not been identified in previous searches with IPC/*Einstein*, HRI/*ROSAT*, ACIS-S/*Chandra*, or EPIC/*XMM-Newton*. After cross-matching with optical and near-infrared catalogues, we classified the X-ray sources into 84 young cluster members and candidates, four active field stars, and 19 galaxies, of which only two have known optical and near-infrared counterparts. Among the cluster members and candidates, two are *bona fide* brown dwarfs with signposts of youth.

A robust Poisson- χ^2 analysis to search for X-ray variability showed that at least seven young stars displayed flares during the HRC-I observations, while two (or three, if we include the B2Vpe star No. 2/Mayrit 42062 AB – σ Ori E) may display rotational modulation. Some of the observed flares were intense, with peak-to-quiescence ratios of about six and durations longer than 20 ks (and longer than our observations in one case).

We compared the count rates and variability status of our HRC-I sources with the results of previous observations with *Einstein*, *ROSAT*, *Chandra*, and *XMM-Newton*, and found that eleven stars displayed significant X-ray flux variations between our observations and others, mostly ascribed to flaring activity. Interestingly, during the HRC-I observations, the brown dwarf No. 84/Mayrit 433123 (S Ori 25) underwent an X-ray brightening by a factor five with respect to the EPIC/*XMM-Newton* epoch. Besides, we revisited old *ROSAT* data and found new flaring activity in the σ Orionis star No. 37/Mayrit 102101 AB. To facilitate further studies, we also compiled the *ROSAT* sources presented by Wolk (1996). From this compilation, we noticed that he tabulated X-ray emission from the brown dwarf Mayrit 433123, but he was not able to classify it as one of the first discovered substellar objects.

The X-ray luminosity function that we presented here ranges from spectral type O9.5V, which corresponds to a mass of about $18 M_{\odot}$, to M6.5, below the hydrogen burning mass limit at $0.07 M_{\odot}$. We found a tendency of early-type stars in multiple systems or with spectral peculiarities to display X-ray emission. On the other side of the luminosity function, the two detected brown dwarfs and the least massive young star candidate are among the σ Orionis members with the highest values of L_X/L_J luminosity ratios. We found X-ray emission from only two stars in the spectral type interval from early A to intermediate-late G.

We noticed that most of the σ Orionis T Tauri stars with the largest infrared excesses have not been detected in X-ray surveys in the area, which supports the scenario of a lower frequency and intensity of X-ray emission of classical (accreting) T Tauri stars than weak-line (non-accreting) T Tauri stars. The only very red ($J - K_s > 1.5$ mag) young star detected with HRC-I/*Chandra* was No. 45/Mayrit 609206, which is a classical T Tauri star with a strong H α emission for its spectral type (K7.0), photometric variability, and a spectral energy distribution typical of Class II objects.

Finally, we investigated the spatial distribution of the X-ray cluster members, which is strongly affected by the degradation of the sensitivity towards the borders of the HRC-I detector. While roughly all the X-ray sources with count rates $CR > 0.1 \text{ ks}^{-1}$ at less than 4 arcmin to the cluster centre were detected, the estimated numbers of missed X-ray clus-

ter members in the 4–10 and 10–20 arcmin annuli are 30 and 100, respectively. Since the core of σ Orionis extends up to 20 arcmin from the centre, defined by the Trapezium-like σ Ori system, additional de-centred pointings with HRC-I/*Chandra*, EPIC/*XMM-Newton*, or the future Wide Field Imager + Hard X-ray Imager instruments onboard the ESA-NASA-JAXA space mission *International X-ray Observatory* are necessary to investigate the full X-ray luminosity function of the cluster. To conclude, a few shallow pointings around the cluster centre will probably be more efficient to detect and characterise new X-ray young brown dwarfs in σ Orionis than a single deep pointing centred on the Trapezium-like system.

Acknowledgements. We are indebt to the anonymous referee for his/her quick, polite, greatly valuable report. JAC is an *investigador Ramón y Cajal* at the CAB, JFAC is a researcher of the Consejo Nacional de Investigaciones Científicas y Tecnológicas (CONICET) at the UNComa, and JLS is an AstroCAM post-doctoral fellow at the UCM. This research made use of the SIMBAD, operated at Centre de Données astronomiques de Strasbourg, France, and NASA's Astrophysics Data System. PWDetect has been developed by scientists at Osservatorio Astronomico di Palermo. Financial support was provided by the Universidad Complutense de Madrid, the Comunidad Autónoma de Madrid, the Spanish Ministerio de Ciencia e Innovación, the Secretaría de Ciencia y Tecnología de la Universidad Central de Córdoba, and the Argentinian CONICET under grants AyA2008-06423-C03-03, AyA2008-00695, PRICIT S-2009/ESP-1496, and PICT 2007-02177.

References

- Adams, N., Wolk, S., Walter, F. M., Jeffries, R., Naylor, T. 2002, American Astronomical Society Meeting 201, #46.08; Bulletin of the American Astronomical Society, Vol. 34, p.1176
- Adams-Wolk, N. R., Wolk, S. J., Walter, F. M. et al. 2002, American Astronomical Society Meeting 203, #77.06; Bulletin of the American Astronomical Society, Vol. 35, p.1324
- Adams, N. R., Wolk, S. J., Walter, F. M., Sherry, W. H. 2004, American Astronomical Society Meeting 205, #105.08; Bulletin of the American Astronomical Society, Vol. 36, p.1518
- Adams-Wolk, N. R., Wolk, S. J., Walter, F. M., Sherry, W. H. 2005, Protostars and Planets V, Proceedings of the Conference held October 24–28, 2005, in Hilton Waikoloa Village, Hawai'i. LPI Contribution No. 1286., p.8425
- Albacete-Colombo, J. F., Caramazza, M., Flaccomio, E., Micela, G., Sciortino, S. 2007, A&A, 474, 495
- Albacete-Colombo, J. F., Damiani, F., Micela, G., Sciortino, S., Harnden, F. R., Jr. 2008, A&A, 490, 1055
- Anders, E., Grevesse, N. 1989, Geochimica et Cosmochimica Acta 53, 197
- Andrews, S. M., Reipurth, B., Bally, J., Heathcote, S. R. 2004, ApJ, 606, 353
- Barrado y Navascués, D., Martín, E. L. 2003, AJ, 126, 2997
- Barrado y Navascués, D., Béjar, V. J. S., Mundt, R. et al. 2003, A&A, 404, 171
- Béjar, V. J. S., Zapatero Osorio, M. R., Rebolo, R. 1999, ApJ, 521, 671
- Béjar, V. J. S., Martín, E. L., Zapatero Osorio, M. R. et al. 2001, ApJ, 556, 830
- Béjar, V. J. S., Zapatero Osorio, M. R., Rebolo, R. 2004, AN, 325, 705
- Bihain, G., Rebolo, R., Zapatero Osorio, M. R. et al. 2009, A&A, 506, 1169

- Bolton, C. T. 1974, *ApJ*, 192, L7
- Bouy, H., Huélamo, N., Martín, E. L. et al. 2009, *A&A*, 493, 931
- Broos, P. S., Feigelson, E. D., Townsley, L. K. et al. 2007, *ApJs*, 169, 353
- Burningham, B., Naylor, T., Littlefair, S. P., Jeffries, R. D. 2005, *MNRAS*, 356, 1583
- Caballero, J. A. 2005, *AN*, 326, 1007
- Caballero, J. A. 2006, Ph.D. Thesis, Universidad de La Laguna, Spain
- Caballero, J. A. 2007a, *A&A*, 466, 917
- Caballero, J. A. 2007b, *AN*, 328, 917
- Caballero, J. A. 2008a, *MNRAS*, 383, 375
- Caballero, J. A. 2008b, *MNRAS*, 383, 750
- Caballero, J. A. 2008c, *A&A*, 478, 667
- Caballero, J. A. 2009, Multi-wavelength Astronomy and Virtual Observatory, Proceedings of the EURO-VO Workshop, held at the European Space Astronomy Centre of ESA, Villafranca del Castillo, Spain, 1-3 December, 2008, Eds.: D. Baines and P. Osuna, Published by the European Space Agency., p.3
- Caballero, J. A. 2010, *A&A*, 514, A18
- Caballero, J. A., Dinis, L. 2008, *AN*, 329, 801
- Caballero, J. A., Béjar, V. J. S., Rebolo, R., Zapatero Osorio, M. R. 2004, *A&A*, 424, 857
- Caballero, J. A., Martín, E. L., Dobbie, P. D. et al. 2006, *A&A*, 460, 635
- Caballero, J. A., Béjar, V. J. S., Rebolo, R. et al. 2007, *A&A*, 470, 903
- Caballero, J. A., Valdivielso, L., Martín, E. L. et al. 2008, *A&A*, 491, 515
- Caballero, J. A., López-Santiago, J., de Castro, E., Cornide, M. 2009, *AJ*, 137, 5012
- Catalano, F. A., Renson, P. 1998, *A&AS*, 127, 421
- Condon, J. J., Cotton, W. D., Greisen, E. W. et al. 1998, *AJ*, 115, 1693
- Daemgen, S., Siegler, N., Reid, I. N., Close, L. M. 2007, *ApJ*, 654, 558
- Damiani, F., Maggio, A., Micela, G., Sciortino, S. 1997a, *ApJ*, 483, 350
- Damiani, F., Maggio, A., Micela, G., Sciortino, S. 1997b, *ApJ*, 483, 370
- Della Ceca, R., Maccacaro, T., Caccianiga, A. et al. 2004, *A&A*, 428, 383
- Drake, S. A. 1990, *AJ*, 100, 572
- Epchtein, N., de Batz, B., Capovani, L. et al. 1997, *Msngr*, 87, 27
- Feigelson, E. D., Casanova, S., Montmerle, T., Guibert, J. 1993, *ApJ*, 416, 623
- Feigelson, E. D., Broos, P., Gaffney, J. A., III et al. 2002, *ApJ*, 574, 258
- Flaccomio, E., Micela, G., Sciortino, S. 2006, *A&A*, 455, 903
- Franciosini, E., Pallavicini, R., Sanz-Forcada, J. 2006, *A&A*, 446, 501
- Frost, E. B., Adams, W. S. 1904, *ApJ*, 19, 151
- Garrison, R. F. 1967, *PASP*, 79, 433
- Gatti, T., Natta, A., Randich, S., Testi, L., Sacco, G. 2008, *A&A*, 481, 423
- Getman, K. V., Feigelson, E. D., Townsley, L. et al. 2002, *ApJ*, 575, 354
- González Hernández, J. I., Caballero, J. A., Rebolo, R. et al. 2008, *A&A*, 490, 1135
- Groote, D., Schmitt, J. H. M. M. 2004, *A&A*, 418, 235
- Güdel, M., Nazé, Y. 2009, *A&ARv*, 17, 309
- Harris, D. E., Forman, W., Gioia, I. M. et al. 1994, *Vizie Online Catalogue IX/13*
- Hernández, J., Hartmann, L., Megeath, T. et al. 2007, *ApJ*, 662, 1067
- Hodapp, K. W., Iserlohe, C., Stecklum, B., Krabbe, A. 2009, *ApJ*, 701, L100
- Jeffries, R. D., Maxted, P. F. L., Oliveira, J. M., Naylor, T. 2006, *MNRAS*, 371, L6
- Joncas, G., Borra, E. F. 1981, *A&A*, 94, 134
- Kenyon, M. J., Jeffries, R. D., Naylor, T., Oliveira, J. M., Maxted, P. F. L. 2005, *MNRAS*, 356, 89
- Kudritzki, R.-P., Puls, J. 2000, *ARA&A*, 38, 613
- Lee, T. A. 1968, *ApJ*, 152, 913
- López-Santiago, J., Caballero, J. A. 2008, *A&A*, 491, 961
- Lucy, L. B., White, R. L. 1980, *ApJ*, 241, 300
- Luhman, K. L., Hernández, J., Downes, J. J., Hartmann, L., Briceño, C. 2008, *ApJ*, 688, 362
- Maggio, A., Flaccomio, E., Favata, F. et al. 2007, *ApJ*, 660, 1462
- Mayne, N. J., Naylor, T. 2008, *MNRAS*, 386, 261
- Maxted, P. F. L., Jeffries, R. D., Oliveira, J. M., Naylor, T., Jackson, R. J. 2008, *MNRAS*, 385, 2210
- Micela, G., Sciortino, S., Harnden, F. R., Jr. et al. 1999, *A&A*, 341, 751
- Mohanty, S., Basri, G., Shu, F., Allard, F., Chabrier, G. 2002, *ApJ*, 571, 469
- Monet, D. G., Levine, S. E., Canzian, B. et al. 2003, *AJ*, 125, 984
- Moran, E. C., Helfand, D. J., Becker, R. H., White, R. L. 1996, *ApJ*, 461, 127
- Morrison, R., McCammon, D. 1983, *ApJ*, 270, 119
- Muzerolle, J., Hillenbrand, L., Calvet, N., Briceño, C., Hartmann, L. 2003, *ApJ*, 592, 266
- Naylor, T. 2009, *MNRAS*, 399, 432
- Neuhäuser, R., Sterzik, M. F., Schmitt, J. H. M. M., Wichmann, R., Krautter, J. 1995, *A&A*, 297, 391
- North, P. 1984, *A&A*, 141, 328
- Oliveira, J. M., Jeffries, R. D., van Loon, J. Th., Rushton, M. T. 2006, *MNRAS*, 369, 272
- Owoccki, S. P., Cohen, D. H. 1999, *ApJ*, 520, 833
- Preibisch, T., Zinnecker, H. 2002, *AJ*, 123, 1613
- Randich, S., Schmitt, J. H. M. M., Prosser, C. F., Stauffer, J. R. 1996, *A&A*, 305, 785
- Reid, N. 2003, *MNRAS*, 342, 837
- Reipurth, B., Bally, J., Fesen, R. A., Devine, D. 1998, *Nature*, 396, 343
- Sacco, G. G., Randich, S., Franciosini, E., Pallavicini, R., Palla, F. 2007, *A&A*, 462, L23
- Sacco, G. G., Franciosini, E., Randich, S., Pallavicini, R. 2008, *A&A*, 488, 167
- Sanz-Forcada, J., Franciosini, E., Pallavicini, R. 2004, *A&A*, 421, 715
- Scholz, A., Eislöffel, J. 2004, *A&A*, 419, 249
- Sherry, W. H., Walter, F. M., Wolk, S. J. 2004, *AJ*, 128, 2316
- Sherry, W. H., Walter, F. M., Wolk, S. J., Adams, N. R. 2008, *AJ*, 135, 1616
- Skinner, S. L., Sokal, K. R., Cohen, D. H. et al. 2008, *ApJ*, 683, 796
- Skrutskie, M. F., Cutri, R. M., Stiening, R. et al. 2006, *AJ*, 131, 1163
- Smith, R. K., Brickhouse, N. S., Liedahl, D. A., Raymond, J. C. 2001, *ApJ*, 556, L91
- Stauffer, J. R., Caillault, J.-P., Gagné, M., Prosser, C. F., Hartmann, L. W. 1994, *ApJs*, 91, 625
- Stelzer, B., Micela, G., Flaccomio, E., Neuhäuser, R., Jayawardhana, R. 2006, *A&A*, 448, 293
- Stelzer, B., Flaccomio, E., Briggs, K. et al. 2007, *A&A*, 468, 463
- Stelzer, B., Scholz, A., Argiroffi, C., Micela, G. 2010, *MNRAS*, accepted, eprint arXiv:1006.2717
- Stern, R. A., Schmitt, J. H. M. M., Kahabka, P. T. 1995, *ApJ*, 448, 683
- Telleschi, A., Güdel, M., Briggs, K. R., Audard, M., Palla, F. 2007, *A&A*, 468, 425
- Townsend, R. H. D., Oksala, M. E., Cohen, D. H., Owoccki, S. P., ud-Doula, A. 2010, *ApJ*, 714, L318
- van Loon, J. Th., Oliveira, J. M. 2003, *A&A*, 405, L33
- Walborn, N. R. 1974, *ApJ*, 191, L95

- White N.E., Giommi P., Angelini L. 2000, Vizie Online Catalogue IX/31
- Wolk, S. J. 1996, Ph.D. Thesis, University of New York at Stony Brook, USA
- Wolk, S. J., Harnden, F. R., Jr., Flaccomio, E. et al. 2005, *ApJs*, 160, 423
- Zapatero Osorio, M. R., Béjar, V. J. S., Martín, E. L. et al. 2000, *Science*, 290, 103
- Zapatero Osorio, M. R., Béjar, V. J. S., Martín, E. L. et al. 2002, *ApJ*, 578, 536
- Zapatero Osorio, M. R., Béjar, V. J. S., Bihain, G. et al. 2008, *A&A*, 477, 895

Appendix A: HRC-I/*Chandra* compared to other X-ray space missions

A.1. IPC/Einstein

We identified the eight 2E sources detected at less or about 15 arcmin to the cluster centre with the Imaging Proportional Counter (IPC) onboard *Einstein* (Harris et al. 1994). Given the large *Einstein* position errors of 30–50 arcsec tabulated in the 2E catalogue, the origin of each X-ray source can be a combination of several bright sources (e.g., 2E 1470 = σ Ori AB + D + E + IRS1 AB). Besides, there was a ninth 2E source at about 16 arcsec to the cluster centre, 2E 1483, which we associated to our HRC-I source No. 99. The *Einstein* Two-Sigma catalogue (Moran et al. 1996) only provided the marginal detection of three additional *ROSAT* sources (Mayrit 528005 AB, Mayrit 653170, and Mayrit 306125 AB) and five possible spurious X-ray detections and, hence, we did not use it.

A.2. HRI/*ROSAT*

We recovered in our HRC-I observations all except one of the 24 sources (23 young stars and the galaxy 2E 1456) detected by Caballero et al. (2009) with the High Resolution Imager (HRI) onboard *ROSAT*. The exception was the flaring star Mayrit 969077 (2E 1487), the most separated X-ray source to the cluster centre in the HRI observation, which fell out of the HRC-I field of view. Of the 23 sources, eight were reported to vary by Caballero et al. (2009). In their variability study, the authors imposed a minimum number of associated X-ray events of $N = 20$. In the present work, we revisited their HRI/*ROSAT* dataset and applied the same methodology as in Caballero et al. (2009) to eight X-ray sources with $5 < N < 20$ not investigated by them. The results of this analysis are summarised in Table A.1. The eight X-ray sources correspond to the active field star No. 31 ([W96] 4771–1056; Section 2.5.2) and seven young σ Orionis stars, of which two are variable according to the robust Poisson- χ^2 criterion in Caballero et al. (2009). The two (highly) variable stars are No. 4 (Mayrit 348349, Haro 5–13), the strong $H\alpha$ emitter that showed the flare decay during the HRC-I observations, and No. 37 (Mayrit 102101 AB, [W96] rJ053851–20130236), an M3-type, accreting, double-lined spectroscopic binary (Wolk 1996; Sacco et al. 2008; Caballero et al. 2008). In both cases, flaring activity was responsible for the large variation in count rates (of up to a factor ten).

Table A.1. X-ray parameters of faint HRI/*ROSAT* sources in σ Orionis not listed by Caballero et al. (2009)^a.

No.	Name	N	\overline{CR} [ks ⁻¹]	σ_{CR} [ks ⁻¹]	$\overline{\delta CR}$ [ks ⁻¹]	χ^2
4	Mayrit 348349	11	11.46	10.03	1.95	114.6
16	Mayrit 97212	11	3.66	0.95	1.22	0.361
18	Mayrit 403090	16	5.07	1.75	1.58	4.663
27	Mayrit 489165	6	2.77	1.68	1.24	2.176
29	Mayrit 92149 AB	6	3.24	1.01	0.77	1.540
31	[W96] 4771–1056	6	3.76	1.00	1.09	1.126
32	Mayrit 374056	13	5.61	1.88	1.88	4.617
37	Mayrit 102101 AB	7	7.77	4.86	1.77	45.91

^a Number of associated X-ray events, mean and standard deviation of the net count rate, mean of the error on the count rate, and normalized double-weighted χ^2 of the X-ray series (see Table 1 in Caballero et al. 2009).

For completeness, in Table C.3 we present a reappraisal of the X-ray sources near σ Ori in the novel work by Wolk (1996). Years later, his work is acknowledged as a cornerstone in the study of the σ Orionis cluster. In the table, we list the names and spectral types¹² of the optical counterparts and coordinates and count rates of the X-ray sources from Wolk (1996), coordinates of the near-infrared counterparts from 2MASS, identification number in our work, and recommended name.

Among the 58 X-ray sources listed in Table C.3, there are three double and one triple detections (including σ Ori AB), between two and four probable spurious detections (marked with ellipses and question marks), two galaxies (No. 9/2E 1456 and No. 62), and three field active stars (No. 31/[W96] 4771–1056, No. 51/[SWW2004] 166, and “R053930–0238”/[SWW2004] 222 AB). The remaining sources correspond to young objects in the σ Orionis cluster. A few sources were not detected in the *Chandra* images, mostly due to the difference in sizes of fields of view.

Interestingly, Wolk (1996) tabulated at $0.81 \pm 0.19 \text{ ks}^{-1}$ the count rate of the X-ray source “R053908–0239” (No. 84/Mayrit 433123), which is the young *brown dwarf* S Ori 25 (see Section 3.3.2). This was the first report of X-ray emission from a substellar object. Unfortunately, Wolk (1996) did not collect optical or near-infrared photometry of the object and could not classify it.

A.3. ACIS-S/*Chandra*

Of the 42 X-ray sources detected with ACIS-S/*Chandra* by Skinner et al. (2008), 40 were HRC-I/*Chandra* X-ray sources with significance of detection larger than 5.4 (Table C.1). One of the other two sources, the X-ray galaxy [SSC2008] 40

¹² Symbols “x” and “...” in the spectral type column in Table C.3 indicate that the stars were spectroscopically investigated by Wolk (1996) but their spectral types were not given and that the stars were not spectroscopically investigated, respectively.

Table A.2. Optical/near-infrared counterparts of EPIC/*XMM-Newton* sources in Franciosini et al. (2006) not listed in Tables 4 or C.1.

NX (Fr06)	α (J2000)	δ (J2000)	CR [ks ⁻¹]	Name	Class
4	05 38 00.56	-02 45 09.7	9.7±1.0	Mayrit 861230	Possible young star
6	05 38 06.50	-02 28 49.4	0.67±0.18	Mayrit 717307	Young star
7	05 38 06.74	-02 30 22.8	19.0±0.9	Mayrit 662301	Young star
11	05 38 13.20	-02 26 08.8	1.6±0.3	Mayrit 757321	Young star
14	05 38 15.53	-02 42 05.1	2.7±0.4	[FPS2006] NX 14	Possible galaxy
17	05 38 17.78	-02 40 50.1	0.97±0.17	Mayrit 498234	Young star
25	05 38 23.32	-02 44 14.2	0.85±0.17	Mayrit 589213	Young star
26	05 38 23.55	-02 41 31.8	0.96±0.19	Mayrit 459224	Young star
33	05 38 27.51	-02 35 04.2	1.5±0.4	Mayrit 265282	Young star
42	05 38 30.98	-02 34 03.8	0.64±0.13	[FPS2006] NX 42	Possible field star
47	05 38 32.68	-02 31 15.6	0.57±0.13	[KJN2005] 3.01 325	Field star
50	05 38 33.02	-02 39 27.9	0.53±0.11	[FPS2006] NX 50	Possible field star?
67	05 38 39.13	-02 28 00.4	1.3±0.2	Mayrit 487350	Young brown dwarf
82	05 38 45.98	-02 45 23.2	0.73±0.18	Mayrit 563178	Possible young star
89	05 38 47.66	-02 30 37.4	2.2±0.5	Mayrit 326008	Young star
97 ^a	05 38 49.93	-02 41 22.8	1.08±0.15	Mayrit 332167	Young star
100	05 38 50.39	-02 26 47.7	1.0±0.2	Mayrit 559009	Young star
101	05 38 51.01	-02 27 45.7	0.70±0.17	[KJN2005] 1.02 156 AB	Field star
111	05 38 54.92	-02 28 58.3	0.69±0.16	Mayrit 449020	Young star
114	05 38 56.99	-02 31 25.6	0.65±0.13	SO110979	Field star
116	05 38 58.84	-02 34 13.2	0.63±0.13	[D90] 3	Radiogalaxy
118	05 38 59.23	-02 33 51.4	0.25±0.07	Mayrit 252059	Young star
147	05 39 12.32	-02 30 06.4	2.1±0.4	Mayrit 544049	Possible young star
149	05 39 14.47	-02 28 33.4	10.9±0.6	Mayrit 631045	Possible young star
157	05 39 18.97	-02 30 55.6	3.0±0.4	Mayrit 596059	Young star?
160	05 39 20.97	-02 30 33.5	5.8±0.5	Mayrit 633059	Young star
167	05 39 26.73	-02 26 17.4	2.9±0.6	Mayrit 856047	Young star
169	05 39 50.56	-02 38 27.0	1.8±0.3	[SWW2004] 222 AB	Field star
174	05 39 39.83	-02 33 16.0	19.8±1.0	Mayrit 841079	Young star
175	05 39 39.99	-02 43 09.7	1.9±0.5	Mayrit 931117	Young star

^a Star NX 97 (Mayrit 332167, [SWW2004] 200) has colours, lithium, radial velocity, and H α emission consistent with membership in cluster (Sacco et al. 2008). Its Mayrit number is firstly given here.

(CXO 40), was recovered with our new 10-spurious search (Section 2.7). We did not detect [SSC2008] 39 (CXO 39, [FPS2006] NX 116). It is probably related to the nearby radio source [D90] 3 (Drake 1990; Caballero 2009), which was also tabulated in the National Radio Astronomy Observatory Very Large Array Sky Survey (NVSS at 1465 MHz; Condon et al. 1998). The measured angular separation, $\rho \sim 1.4$ arcsec, is consistent with the large NVSS mean error in declination of more than 6 arcsec. [D90] 3 might be a radio-galaxy with variable X-ray emission.

A.4. EPIC/*XMM-Newton*

In Tables 4 and C.1, there are 87 X-ray sources in common between our observations with HRC-I/*Chandra* and the ones with EPIC/*XMM-Newton* by Franciosini et al. (2006). However, the authors reported 175 detections. Only thirty of the 88 unidentified sources, listed in Table A.2, have optical and near-infrared counterparts. They are 18 σ Orionis stars and brown dwarfs

with signposts of youth, four cluster member candidates, four field stars, two possible field stars, a possible galaxy, and the radiogalaxy [D90] 3. In the table, the uncertainty in the actual stellar counterpart of two X-ray sources is indicated with a question mark. Following the criterion in López-Santiago & Caballero (2008), we classified the other 58 X-ray sources with no 2MASS counterpart as faint active galaxies (the X-ray sources NX 46 and NX 123 had blue optical counterparts in the Guide Star Catalog).

We were able to identify 23 sources not detected by Franciosini et al. (2006). Of them, the authors provided EPIC count-rate upper levels for seven young stars and candidates (marked with the symbol “<” in the NX column in Table C.1). The source No. 25 (Mayrit 3020 AB, σ Ori IRS1), at only 3 arcsec from σ Ori AB, was not resolved by EPIC. Most of the remaining 15 new sources fell at angular separations to the pointing centre larger than $\rho \sim 15$ arcmin (e.g., the bright X-ray galaxy No. 9/2E 1454 or the young star candidate No. 46/Mayrit 1093033) or shorter than $\rho \sim 3$ arcmin (where

the background level due to σ Ori AB in the EPIC observations was high). Among the 23 sources not detected by Franciosini et al. (2006), eight sources were detected independently with ACIS-S by Skinner et al. (2008). There were also eight young stars with signposts of youth, including the early-type stars No. 70/Mayrit 13084 (σ Ori D) and No. 74/Mayrit 182305 (HD 294272 A), six young star candidates, and two galaxies (No. 9/2E 1456 and No. 64/UCM0536–0239, which was also detected by Skinner et al. 2008). They all have low significances of detection in our HRC-I data.

- * No. 96: the 2MASS photometric quality flag of the infrared source close to the X-ray source is EEA, an indication of binarity. Public IRAC/*Spitzer* images resolve the 2MASS source into two point-like sources.
- * No. 97: Mayrit 68191 might be its actual optical counterpart.
- * No. 107: [BNL2005] 1.02 156 may be its actual optical counterpart, which could correspond to the X-ray source [FPS2006] NX 101 (Table A.2).

Appendix C: Long tables

Appendix B: Notes on individual objects

B.1. Notes to Table 1

- * No. 25/Mayrit 3020 AB (σ Ori IRS1 AB) is a Class II (or Class-I proplyd?) binary star located at $\rho = 3.32 \pm 0.06$ arcsec, $\theta = 19.6 \pm 1.4$ deg, to σ Ori AB. In turn, it forms a binary system separated by $\rho \approx 0.24$ arcsec, $\theta \approx 318$ deg (Bouy et al. 2009; Hodapp et al. 2009). Coordinates and *J*-band magnitude of Mayrit 3020 AB are from the unresolved adaptive optics observations in Caballero (2006). The tabulated *H*- and *K_s*-band magnitudes, from Bouy et al. (2009), are for the primary Mayrit 3020 A. The secondary Mayrit 3020 B has *H* = 12.84 ± 0.07 mag and *K_s* = 12.65 ± 0.07 mag.
- * No. 31/[W96] 4771–1056 is a possible field star discovered by Wolk (1996). He derived K1 spectral type and found $H\alpha$ in absorption. The Li I $\lambda 6708$ Å equivalent width was smaller than expected for an early K-type cluster member. The star does not follow the spectro-photometric sequence of the cluster.
- * No. 39/Mayrit 168291 A, No. 47/Mayrit 68229, and No. 57/Mayrit 492211 have lithium absorption, radial velocity, and $H\alpha$ emission consistent with membership in σ Orionis (Sacco et al. 2008). Their Mayrit numbers are firstly given here. No. 39/Mayrit 168291 A has a fainter visual companion, tentatively called Mayrit 168291 B, at about 3.5 arcsec to the northeast. Neither DENIS nor 2MASS resolved the system.
- * No. 58/Mayrit 21023 is located at $\rho \approx 21$ arcsec, $\theta \approx 23$ deg, to σ Ori AB. Their coordinates and *JHK_s* magnitudes are from Caballero (2007b). Besides, the DENIS catalogue tabulates *i* = 14.31 ± 0.03 mag, which seems to be affected by the glare of the nearby σ Ori system.

B.2. Notes to Table 2

- * No. 62: digitisations of the Palomar Optical Sky Survey show an extended source (probably the X-ray host galaxy) in the background of a field dwarf. The brown dwarf cluster member candidate S Ori 43 (Béjar et al. 1999) is also in a 6 arcsec-radius cone search around the X-ray source.
- * No. 93: it has a close, faint, blue, extended, USNO-B1 visual companion. Although this source is probably of extragalactic nature, it does not seem to be the origin of the X-ray source.

Table C.1. HRC-I/*Chandra* X-ray detections with significance larger than 5.1.

No.	α (J2000)	δ (J2000)	$\Delta\alpha, \Delta\delta$ [arcsec]	S (σ)	Offaxis [arcmin]	CR [ks ⁻¹]	Flux [10 ⁻¹⁷ W m ⁻²]	NX (Fr06)	CXO (Sk08)
1	05 38 44.76	-02 36 00.1	0.04	423	0.26	286.6 \pm 1.8	261.1	80	19
2	05 38 38.49	-02 34 55.1	0.11	170	2.05	47.7 \pm 0.8	44.7	65	10
3	05 38 47.19	-02 35 40.3	0.11	145	0.43	29.5 \pm 0.6	26.3	84	23
4	05 38 40.28	-02 30 18.7	0.40	142	5.74	48.5 \pm 0.9	43.6	69	...
5	05 38 53.37	-02 33 23.1	0.22	131	3.15	27.7 \pm 0.6	24.0	109	37
6	05 38 44.22	-02 32 33.7	0.22	130	3.35	28.3 \pm 0.6	25.5	79	...
7	05 37 53.09	-02 33 34.2	2.02	123	13.3	91.3 \pm 1.4	106.3	2	...
8	05 39 36.48	-02 42 17.5	2.02	112	14.2	100.8 \pm 1.7	108.8	172	...
9	05 37 56.34	-02 45 11.9	2.12	105	15.4	101.8 \pm 1.9	119.2
10	05 39 01.48	-02 38 56.3	0.47	99.8	4.98	20.9 \pm 0.5	18.5	125	42
11	05 38 43.55	-02 33 25.4	0.11	97.7	2.53	21.1 \pm 0.7	21.0	76	...
12	05 38 38.22	-02 36 38.2	0.11	93.5	2.01	14.3 \pm 0.4	13.3	64	9
13	05 38 32.84	-02 35 39.1	0.18	92.2	3.22	18.6 \pm 0.5	16.4	49	4
14	05 37 54.40	-02 39 29.6	1.66	92.0	13.3	63.6 \pm 1.4	74.3	3	...
15	05 38 44.24	-02 40 19.3	0.36	86.2	4.45	15.0 \pm 0.4	13.5	78	18
16	05 38 41.29	-02 37 22.4	0.14	79.8	1.85	10.1 \pm 0.3	9.3	70	13
17	05 38 49.18	-02 38 22.0	0.14	69.6	2.62	9.5 \pm 0.4	9.5	93	29
18	05 39 11.62	-02 36 02.7	0.72	68.1	6.47	15.5 \pm 0.5	14.4	145	...
19	05 38 07.87	-02 31 31.3	1.87	66.4	10.4	27.8 \pm 0.8	33.5	8	...
20	05 38 35.87	-02 30 43.4	0.54	65.5	5.72	13.1 \pm 0.5	12.2	62	...
21	05 38 48.00	-02 27 14.1	1.37	65.4	8.68	21.9 \pm 0.6	21.4	90	...
22	05 38 35.45	-02 31 51.7	0.43	52.4	4.77	8.5 \pm 0.3	7.6	60	...
23	05 38 48.69	-02 36 16.1	0.11	52.0	0.83	4.6 \pm 0.2	4.5	92	27
24	05 38 35.22	-02 34 38.0	0.18	50.9	2.91	6.9 \pm 0.5	7.1	58	8
25	05 38 44.84	-02 35 57.1	0.11	48.8	0.22	4.1 \pm 0.2	4.7	(80)	20
26	05 38 47.46	-02 35 25.3	0.18	48.3	0.64	3.9 \pm 0.2	3.5	87	24
27	05 38 53.18	-02 43 52.6	1.15	46.2	8.20	12.8 \pm 0.5	13.3	106	...
28	05 38 35.87	-02 43 50.4	1.15	45.4	8.32	12.2 \pm 0.5	14.0	61	...
29	05 38 47.90	-02 37 19.2	0.18	43.1	1.53	3.07 \pm 0.19	2.91	88	25
30	05 39 07.58	-02 32 39.0	0.90	41.9	6.35	7.4 \pm 0.4	7.5	138	...
31	05 39 00.53	-02 39 38.8	0.65	41.1	5.27	5.9 \pm 0.3	5.9	122	41
32	05 39 05.39	-02 32 30.2	0.90	38.6	5.97	6.3 \pm 0.3	6.3	132	...
33	05 39 18.05	-02 29 29.1	2.30	37.6	10.3	15.2 \pm 0.7	20.3	156	...
34	05 38 34.23	-02 34 16.0	0.36	36.7	3.30	3.3 \pm 0.2	2.9	55	...
35	05 38 54.09	-02 49 29.8	3.17	34.4	13.8	23.9 \pm 1.2	41.3	110	...
36	05 38 31.57	-02 35 14.9	0.40	33.8	3.59	2.64 \pm 0.19	2.68	44	3
37	05 38 51.45	-02 36 20.3	0.14	33.2	1.50	2.08 \pm 0.16	2.19	102	33
38	05 38 29.12	-02 36 02.5	0.40	33.1	4.14	3.1 \pm 0.2	3.2	39	1
39	05 38 34.32	-02 35 00.1	0.22	32.7	2.98	3.0 \pm 0.3	3.5	56	7
40	05 38 52.00	-02 46 43.4	2.41	32.2	11.0	12.8 \pm 0.7	23.0	104	...
41	05 38 45.36	-02 41 58.8	0.97	32.0	6.09	4.5 \pm 0.3	5.0	81	21
42	05 38 26.43	-02 34 28.3	0.76	28.6	5.02	3.2 \pm 0.2	3.1	31	...
43	05 38 50.04	-02 37 35.4	0.22	26.3	2.01	1.38 \pm 0.13	1.45	98	31
44	05 39 32.41	-02 39 44.1	2.70	23.9	12.3	11.3 \pm 0.8	20.9	170	...
45	05 38 27.32	-02 45 09.0	2.77	23.2	10.3	8.1 \pm 0.6	15.5	32	...
46	05 39 24.39	-02 20 45.2	3.74	23.0	18.0	32 \pm 3	62
47	05 38 41.36	-02 36 44.3	0.18	20.8	1.37	0.96 \pm 0.12	0.92	71	14
48	05 38 33.35	-02 36 17.4	0.47	19.9	3.11	1.20 \pm 0.13	1.19	52	5
49	05 38 51.75	-02 36 03.2	0.25	18.8	1.52	0.87 \pm 0.10	0.80	103	34
50	05 39 02.74	-02 29 55.8	1.22	17.6	7.32	3.5 \pm 0.4	3.3	126	...
51	05 38 53.06	-02 38 53.4	0.36	17.2	3.52	0.91 \pm 0.11	0.98	105	36
52	05 38 48.29	-02 36 40.9	0.22	17.2	1.02	0.74 \pm 0.10	0.65	91	26

Table C.1. HRC-I/*Chandra* X-ray detections with significance larger than 5.1 (cont.).

No.	α (J2000)	δ (J2000)	$\Delta\alpha, \Delta\delta$ [arcsec]	S (σ)	Offaxis [arcmin]	CR [ks ⁻¹]	Flux [10 ⁻¹⁷ W m ⁻²]	NX (Fr06)	CXO (Sk08)
53	05 39 14.99	-02 31 37.4	1.69	16.4	8.47	4.1 \pm 0.4	6.0	150	...
54	05 38 49.23	-02 41 24.8	1.26	16.2	5.59	1.9 \pm 0.2	2.6	94	28
55	05 38 59.05	-02 47 12.7	3.24	15.2	11.8	7.0 \pm 0.7	14.9	117	...
56	05 38 38.72	-02 30 21.2	1.33	14.7	5.81	1.7 \pm 0.2	1.6	66	...
57	05 38 27.74	-02 43 00.9	1.76	14.4	8.42	3.0 \pm 0.3	4.7	34	...
58	05 38 45.31	-02 35 41.1	0.29	14.0	0.23	0.53 \pm 0.08	0.69
59	05 38 42.28	-02 37 14.6	0.22	14.0	1.60	0.52 \pm 0.08	0.54	<	15
60	05 38 34.05	-02 36 37.2	0.40	14.0	3.00	0.67 \pm 0.10	0.79	54	6
61	05 38 43.02	-02 36 14.3	0.22	13.7	0.75	0.46 \pm 0.08	0.51	...	16
62	05 38 13.85	-02 35 00.1	2.56	13.3	7.99	3.1 \pm 0.4	7.0	<	...
63	05 38 59.65	-02 45 08.2	3.46	13.2	9.88	4.5 \pm 0.5	11.0	119	...
64	05 38 41.23	-02 37 37.6	0.29	13.0	2.06	0.51 \pm 0.08	0.56	...	12
65	05 38 43.31	-02 32 00.9	0.58	12.6	3.92	0.92 \pm 0.16	0.91	75	...
66	05 39 22.81	-02 33 34.0	2.59	11.8	9.55	3.7 \pm 0.5	6.9	161	...
67	05 38 46.85	-02 36 43.4	0.22	11.7	0.88	0.31 \pm 0.06	0.38	<	22
68	05 38 58.27	-02 38 51.3	0.79	11.7	4.32	0.86 \pm 0.13	0.70	115	38
69	05 38 29.87	-02 23 38.4	3.96	9.72	12.9	5.4 \pm 0.9	14.0	41	...
70	05 38 45.63	-02 35 58.7	0.25	9.60	0.09	0.33 \pm 0.09	0.29
71	05 38 08.26	-02 35 56.0	2.95	8.97	9.35	2.1 \pm 0.3	5.0	9	...
72	05 38 33.60	-02 44 13.5	2.20	8.87	8.86	1.7 \pm 0.3	3.3	53	...
73	05 39 05.17	-02 33 00.7	0.68	8.54	5.65	0.48 \pm 0.13	0.66	131	...
74	05 38 34.79	-02 34 15.8	0.65	8.48	3.17	0.45 \pm 0.12	0.39
75	05 39 25.20	-02 38 22.4	3.02	8.44	10.2	2.6 \pm 0.5	7.3	165	...
76	05 38 51.88	-02 33 32.6	0.36	8.42	2.81	0.30 \pm 0.09	0.26	...	35
77	05 37 51.59	-02 35 26.7	4.32	8.39	13.5	3.1 \pm 0.6	10.9	1	...
78	05 38 50.80	-02 36 26.6	0.36	8.31	1.39	0.28 \pm 0.09	0.33	<	...
79	05 38 31.41	-02 36 33.7	0.65	8.20	3.63	0.45 \pm 0.12	0.47	<	2
80	05 39 11.60	-02 31 05.3	3.17	7.94	8.06	2.0 \pm 0.4	5.4	144	...
81	05 39 01.17	-02 36 39.1	0.90	7.76	3.94	0.55 \pm 0.14	0.68	124	...
82	05 38 18.35	-02 35 38.3	1.69	7.65	6.84	1.0 \pm 0.3	2.4	19	...
83	05 39 01.05	-05 33 38.5	0.68	7.62	4.44	0.55 \pm 0.14	0.53
84	05 39 08.98	-02 39 58.6	1.73	7.34	7.10	1.0 \pm 0.3	1.8	140	...
85	05 38 39.73	-02 40 19.7	0.68	7.20	4.68	0.38 \pm 0.11	0.51	68	11
86	05 38 36.87	-02 36 43.2	0.40	7.12	2.36	0.23 \pm 0.07	0.15	<	...
87	05 38 20.23	-02 38 02.8	1.80	6.95	6.72	0.9 \pm 0.2	1.7	20	...
88	05 39 45.79	-02 40 35.8	6.37	6.94	15.7	5.6 \pm 1.3	27.5
89	05 39 07.54	-02 28 22.3	4.68	6.89	9.29	2.7 \pm 0.7	9.7	137	...
90	05 39 16.94	-02 25 43.6	4.68	6.88	12.8	3.0 \pm 0.7	11.1	154	...
91	05 38 41.59	-02 28 20.0	1.80	6.85	7.63	0.9 \pm 0.2	1.6	72	...
92	05 38 49.70	-02 34 52.8	0.32	6.70	1.42	0.17 \pm 0.07	0.20	...	30
93	05 38 42.14	-02 43 16.1	2.45	6.65	7.43	1.2 \pm 0.3	3.0	73	...
94	05 38 01.45	-02 25 53.5	6.73	6.41	14.9	4.1 \pm 1.0	29.2
95	05 39 24.42	-02 34 03.1	3.53	6.21	9.84	1.7 \pm 0.5	5.7	164	...
96	05 39 06.66	-02 38 05.0	1.40	5.92	5.67	0.57 \pm 0.16	1.1
97	05 38 43.87	-02 37 06.1	0.25	5.92	1.29	0.12 \pm 0.05	0.18	<	17
98	05 39 33.42	-02 20 37.1	7.02	5.70	19.4	4.8 \pm 1.3	43.1
99	05 39 37.50	-02 26 58.5	7.16	5.62	15.7	3.9 \pm 1.0	25.6	173	...
100	05 38 26.16	-02 29 10.4	2.66	5.51	8.30	1.0 \pm 0.3	2.5	30	...
101	05 38 50.16	-02 36 54.0	0.32	5.42	1.50	0.13 \pm 0.05	0.13	99	32
102	05 38 41.55	-02 39 09.1	0.14	5.41	3.42	0.08 \pm 0.06	0.01
103	05 39 16.91	-02 41 18.1	2.66	5.39	9.49	1.0 \pm 0.3	2.7	153	...
104	05 38 37.36	-02 42 50.0	1.48	5.35	7.23	0.49 \pm 0.15	0.89	63	...
105	05 38 35.58	-02 34 04.5	0.18	5.35	3.11	0.08 \pm 0.05	0.05

Table C.1. HRC-I/*Chandra* X-ray detections with significance larger than 5.1 (cont.).

No.	α (J2000)	δ (J2000)	$\Delta\alpha, \Delta\delta$ [arcsec]	S (σ)	Offaxis [arcmin]	CR [ks ⁻¹]	Flux [10 ⁻¹⁷ W m ⁻²]	NX (Fr06)	CXO (Sk08)
106	05 39 11.14	-02 36 48.1	1.44	5.22	6.42	0.49 \pm 0.15	0.68	143	...
107	05 38 28.43	-02 32 30.7	1.51	5.11	5.48	0.47 \pm 0.15	0.91	35	...

Table C.2. Optical/near-infrared counterparts of X-ray sources in Table C.1.

No.	2MASS designation	Name	Alternative name	Class
1	05384476–0236001	Mayrit AB	σ Ori AB + “F”	Young star
2	05383848–0234550	Mayrit 114305 AB	[W96] 4771–1147 AB	Young star
3	05384719–0235405	Mayrit 42062 AB	σ Ori E + “Eb”	Young star
4	05384027–0230185	Mayrit 348349	Haro 5–13	Young star
5	05385337–0233229	Mayrit 203039	[W96] 4771–1049	Young star
6	05384424–0232336	Mayrit 207358	[W96] 4771–1055	Young star
7	05375303–0233344	Mayrit 789281	2E 1454	Young star
8	05393654–0242171	Mayrit 863116 AB	RX J0539.6–0242 AB	Young star
9	05375630–0245130	2E 1456	2E 0535.4–0246	Galaxy
10	05390149–0238564	Mayrit 306125 AB	HD 37525 AB	Young star
11	05384355–0233253	Mayrit 156353	[SWW2004] 36	Young star
12	05383822–0236384	Mayrit 105249	[W96] rJ053838–0236	Young star
13	05383284–0235392	Mayrit 180277	[W96] rJ053832–0235b	Young star
14	05375440–0239298	Mayrit 783254	2E 1455	Young star
15	05384423–0240197	Mayrit 260182	[W96] 4771–1051	Young star
16	05384129–0237225	Mayrit 97212	[W96] rJ053841–0237	Young star
17	05384917–0238222	Mayrit 157155	[W96] rJ053849–0238	Young star
18	05391163–0236028	Mayrit 403090	[W96] 4771–1038	Young star
19	05380784–0231314	Mayrit 615296	2E 1459	Young star
20	05383587–0230433	Mayrit 344337 AB	[W96] 4771–1097	Young star
21	05384803–0227141	Mayrit 528005 AB	[W96] 4771–0899 AB	Young star
22	05383546–0231516	Mayrit 285331	[W96] rJ053835–0231	Young star
23	05384868–0236162	Mayrit 61105	[SWW2004] 35	Young star
25	05384484–0235571	Mayrit 3020 AB	σ Ori IRS1 AB	Young star
26	05384746–0235252	Mayrit 53049	[SWW2004] 78	Young star
27	05385317–0243528	Mayrit 489165	[SWW2004] 47	Young star
28	05383587–0243512	Mayrit 489196	TY Ori	Young star
29	05384791–0237192	Mayrit 92149 AB	[W96] R053847–0237 AB	Young star
30	05390760–0232391	Mayrit 397060	V507 Ori	Young star
31	05390052–0239390	[W96] 4771–1056	[SSC2008] 41	Possible field star
32	05390540–0232303	Mayrit 374056	[W96] 4771–1075	Young star
33	05391807–0229284	Mayrit 634052	[W96] 4771–0598	Young star
34	05383422–0234160	Mayrit 189303	HD 294272 B	Young star
35	05385410–0249297	Mayrit 822170	RX J0538.9–0249	Young star
36	05383157–0235148	Mayrit 203283	[W96] rJ053831–0235	Young star
37	05385145–0236205	Mayrit 102101 AB	[W96] rJ053851–0236	Young star
38	05382911–0236026	Mayrit 234269	[SWW2004] 177	Young star
39	05383431–0235000	Mayrit 168291 AB	[W96] rJ053834–0234	Young star
40	05385200–0246436	Mayrit 653170	RU Ori	Young star
41	05384537–0241594	Mayrit 359179	V595 Ori	Young star
42	05382639–0234286	SO210038	2MASS J05382639–0234286	Field star
43	05385003–0237354	Mayrit 124140	[W96] pJ053850–0237	Young star candidate
44	05393256–0239440	Mayrit 750107	[W96] rJ053932–0239	Young star
45	05382725–0245096	Mayrit 609206	V505 Ori	Young star
46	05392456–0220441	Mayrit 1093033	[HHM2007] 1030	Young star candidate
47	05384135–0236444	Mayrit 68229	[W96] pJ053841–0236	Young star
48	05383335–0236176	Mayrit 172264	[SWW2004] 130	Young star candidate
49	05385173–0236033	Mayrit 105092	[FPS2006] NX 103	Young star
50	05390276–0229558	Mayrit 453037 AB	[W96] R053902–0229 AB	Young star
51	05385306–0238536	[SWW2004] 166	[OJV2006] 6	Field star
52	05384828–0236409	Mayrit 67128	[FPS2006] NX 91	Young star
53	05391506–0231376	Mayrit 524060	HD 37564	Young star

Table C.2. Optical/near-infrared counterparts of X-ray sources in Table C.1 (cont.).

No.	2MASS designation	Name	Alternative name	Class
54	05384921–0241251	Mayrit 332168 AB	[SWW2004] 205	Young star
55	05385911–0247133	Mayrit 707162	[W96] rJ053859–0247 AB	Young star
57	05382774–0243009	Mayrit 492211	[SWW2004] 87	Young star
58	05384531–0235413	Mayrit 21023	[BHM2009] 14	Young star candidate
59	05384227–0237147	Mayrit 83207	[W96] pJ053842–0237	Young star
60	05383405–0236375	Mayrit 165257	[W96] rJ053833–0236	Young star
61	05384301–0236145	Mayrit 30241	[HHM2007] 687	Young star candidate
63	05385955–0245080	Mayrit 591158	[W96] 4771–0026	Young star
64	05384123–0237377	UCM0536–0239	[HHM2007] 668	Galaxy
65	05384333–0232008	Mayrit 240355 AB	[SWW2004] 144	Young star
66	05392286–0233330	Mayrit 590076	[W96] rJ053923–0233	Young star
67	05384684–0236435	Mayrit 53144	[BNL2005] 3.01–67	Young star
69	05382993–0223381	[W96] rJ053829–0223	SO120731	Field star
70	05384561–0235588	Mayrit 13084	σ Ori D	Young star
71	05380826–0235562	Mayrit 547270 AB	Kiso A–0976 316	Young star
72	05383368–0244141	Mayrit 521199	TX Ori	Young star
73	05390524–0233005	Mayrit 355060	[SWW2004] 175	Young star
74	05383479–0234158	Mayrit 182305	HD 294272 A	Young star
75	05392519–0238220	Mayrit 622103	BG Ori	Young star
77	05375161–0235257	Mayrit 797272	[W96] rJ053751–0235	Young star
78	05385077–0236267	Mayrit 94106	[KJN2005] 8	Young star
79	05383141–0236338	Mayrit 203260	Haro 5–11	Young star
80	05391151–0231065	Mayrit 497054	V509 Ori	Young star
81	05390115–0236388	Mayrit 249099	[KJN2005] 9	Young star
82	05381834–0235385	Mayrit 396273	S Ori J053818.2–023539	Young brown dwarf
84	05390894–0239579	Mayrit 433123	S Ori 25	Young brown dwarf
85	05383972–0240197	Mayrit 270196	[HHM2007] 655	Young star candidate
86	05383687–0236432	Mayrit 126250 AB	[SWW2004] 154 AB	Young star candidate
87	05382021–0238016	Mayrit 387252	S Ori J053820.1–023802	Young star
88	05394619–0240320	Mayrit 960106	V1147 Ori	Young star
89	05390759–0228234	Mayrit 571037	[W96] rJ053907–0228	Young star
90	05391717–0225433	Mayrit 785038	Kiso A–0904 80	Young star
92	05384970–0234526	Mayrit 100048	[HHM2007] 754	Young star
94	05380167–0225527	Mayrit 887313	[SE2004] 53	Young star candidate
95	05392435–0234013	Mayrit 605079	[SWW2004] 127	Young star candidate
98	05393378–0220398	Mayrit 1178039	[SWW2004] 138	Young star candidate
99	05393729–0226567	Mayrit 957055	[SWW2004] 163	Young star candidate
103	05391699–0241171	Mayrit 578123	[FPS2006] NX 153	Young star candidate

Table C.3. A reappraisal to the X-ray sources near σ Ori in Wolk (1996).

Source identification	α_{W096} (J2000)	δ_{W096} (J2000)	CR [ks ⁻¹]	Sp. type	α_{2MASS} (J2000)	δ_{2MASS} (J2000)	No.	Name
R053751–0235	05 37 51.5	–02 35 25	1.49 ± 0.66	M0	05 37 51.61	–02 35 25.7	77	Mayrit 797272
4771 0775	05 37 52.1	–02 40 40	1.20 ± 0.59	K0
4771 0921	05 37 52.7	–02 33 33	13.4 ± 1.13	K0	05 37 53.03	–02 33 34.4	7	Mayrit 789281
R053754–0239	05 37 53.9	–02 39 27	18.2 ± 1.57	...	05 37 54.40	–02 39 29.8	14	Mayrit 783254
R053755–0245	05 37 55.4	–02 45 07	22.4 ± 1.67	...	05 37 56.30	–02 45 13.0	9	2E 1456
	05 37 55.7	–02 45 16	22.4 ± 1.56					
	05 37 56.0	–02 45 12	23.5 ± 1.67					
4771 0947	05 38 06.8	–02 30 30	1.01 ± 0.47	×	05 38 06.74	–02 30 22.8	...	Mayrit 662301
4771 0854	05 38 07.5	–02 31 27	6.31 ± 0.85	...	05 38 07.84	–02 31 31.4	19	Mayrit 615296
R053808–0235	05 38 08.0	–02 35 50	1.14 ± 0.63	K5	05 38 08.26	–02 35 56.2	71	Mayrit 547270 AB
R053813–0234	05 38 13.9	–02 34 57	1.80 ± 0.42	62	...
R053814–0236	05 38 14.6	–02 36 37	0.60 ± 0.14
R053820–0237	05 38 20.3	–02 37 47	2.01 ± 0.47	M0	05 38 20.21	–02 38 01.6	87	Mayrit 387252
R053827–0242	05 38 27.7	–02 42 58	2.25 ± 0.62	...	05 38 27.74	–02 43 00.9	57	Mayrit 492211
R053828–0236	05 38 28.8	–02 36 00	0.95 ± 0.61	K5	05 38 29.11	–02 36 02.6	34	Mayrit 234269
R053831–0235	05 38 31.4	–02 35 04	0.85 ± 0.42	K7	05 38 31.57	–02 35 14.8	36	Mayrit 203283
R053832–0235	05 38 32.7	–02 35 35	3.20 ± 0.78	...	05 38 32.84	–02 35 39.2	13	Mayrit 180277
R053833–0236	05 38 33.7	–02 36 25	0.36 ± 0.69	K5	05 38 34.05	–02 36 37.5	60	Mayrit 165257
R053834–0234	05 38 34.2	–02 34 16	1.60 ± 0.73	K0	05 38 34.22	–02 34 16.0	34	Mayrit 189303
	05 38 34.1	–02 34 18	0.92 ± 0.64					
R053835–0231	05 38 35.2	–02 31 48	8.23 ± 0.95	K5	05 38 35.46	–02 31 51.6	22	Mayrit 285331
4771 1097	05 38 35.7	–02 30 39	3.52 ± 0.76	K5	05 38 35.87	–02 30 43.3	20	Mayrit 344337 AB
R053838–0236	05 38 38.1	–02 36 38	3.44 ± 0.76	K5	05 38 38.22	–02 36 38.4	12	Mayrit 105249
4771 1147	05 38 38.3	–02 34 51	12.1 ± 1.07	K0	05 38 38.48	–02 34 55.0	2	Mayrit 114305
R053840–0230	05 38 39.8	–02 30 17	2.51 ± 0.75	M0	05 38 40.27	–02 30 18.5	4	Mayrit 348349
R053841–0237	05 38 41.2	–02 37 20	3.03 ± 0.75	K3	05 38 41.29	–02 37 22.5	16	Mayrit 97212
R053843–0233	05 38 43.3	–02 33 20	1.23 ± 0.73	...	05 38 43.55	–02 33 25.3	11	Mayrit 156353
4771 1051	05 38 44.0	–02 40 18	6.10 ± 0.84	K5	05 38 44.23	–02 40 19.7	15	Mayrit 260182
4771 1055	05 38 44.1	–02 32 30	7.49 ± 0.92	...	05 38 44.24	–02 32 33.6	6	Mayrit 207358
R053845–0236	05 38 44.6	–02 35 58	120 ± 2.99	O9.5	05 38 44.76	–02 36 00.1	1	Mayrit AB
	05 38 45.4	–02 36 00	130 ± 3.76					
R053845–0241	05 38 45.3	–02 41 58	1.59 ± 0.63	...	05 38 45.37	–02 41 59.4	41	Mayrit 359179
R053847–0235	05 38 47.0	–02 35 35	8.33 ± 1.03	B2	05 38 47.19	–02 35 40.5	3	Mayrit 42062 AB
R053847–0237	05 38 47.6	–02 37 18	2.34 ± 0.80	K5	05 38 47.91	–02 37 19.2	29	Mayrit 92149 AB
4771 0899	05 38 47.6	–02 27 09	4.28 ± 0.93	K3	05 38 48.03	–02 27 14.1	21	Mayrit 528005 AB
R053849–0238	05 38 49.0	–02 38 21	6.40 ± 0.87	K5	05 38 49.17	–02 38 22.2	17	Mayrit 157155
R053851–0236	05 38 51.3	–02 36 15	2.65 ± 0.50	K5	05 38 51.45	–02 36 20.5	37	Mayrit 102101 AB
4771 0080	05 38 51.8	–02 46 41	5.39 ± 0.98	K7	05 38 52.00	–02 46 43.6	40	Mayrit 653170
R053852–0238	05 38 52.7	–02 38 56	1.91 ± 0.62	...	05 38 53.06	–02 38 53.6	51	[SWW2004] 166
R053853–0243	05 38 52.9	–02 43 47	2.88 ± 0.83	×	05 38 53.17	–02 43 52.8	27	Mayrit 489165
4771 1049	05 38 53.2	–02 33 20	12.0 ± 1.08	K5	05 38 53.37	–02 33 22.9	5	Mayrit 203039
4771 0119	05 38 54.2	–02 49 27	4.03 ± 0.90	...	05 38 54.10	–02 49 29.7	35	Mayrit 822170
4771 0226	05 38 59.1	–02 44 59	3.65 ± 0.85	...	05 38 59.55	–02 45 08.0	63	Mayrit 591158
4771 1056	05 39 00.4	–02 39 35	0.65 ± 0.82	K1	05 39 00.52	–02 39 39.0	31	[W96] 4771–1056
R053901–0238	05 39 01.3	–02 38 54	5.96 ± 0.90	B5	05 39 01.49	–02 38 56.4	10	Mayrit 306125 AB
R053901–0240	05 39 01.6	–02 40 57	0.97 ± 0.22	[FPS2006] NX 121 (?)
R053902–0229	05 39 02.6	–02 29 47	2.61 ± 0.61	K7	05 39 02.76	–02 29 55.8	50	Mayrit 453037 AB
4771 1075	05 39 05.3	–02 32 24	2.75 ± 0.73	K5	05 39 05.40	–02 32 30.3	32	Mayrit 374056
4771 1092	05 39 07.4	–02 32 33	3.20 ± 0.75	K3	05 39 07.60	–02 32 39.1	30	Mayrit 397060
R053908–0239	05 39 08.7	–02 39 54	0.81 ± 0.19	...	05 39 08.94	–02 39 57.9	84	Mayrit 433123
4771 0901	05 39 11.3	–02 30 59	1.89 ± 0.44	K5	05 39 11.51	–02 31 06.5	80	Mayrit 497054
4771 1038	05 39 11.6	–02 35 58	1.67 ± 0.69	K5	05 39 11.63	–02 36 02.8	18	Mayrit 403090

Table C.3. A reappraisal to the X-ray sources near σ Ori in Wolk (1996) (cont.).

Source identification	α_{W096} (J2000)	δ_{W096} (J2000)	CR [ks ⁻¹]	Sp. type	α_{2MASS} (J2000)	δ_{2MASS} (J2000)	No.	Name
R053914–0228	05 39 14.8	–02 28 27	1.48 ± 0.62	...	05 39 14.47	–02 28 33.4	...	Mayrit 631045
R053916–0233	05 39 16.8	–02 33 03	0.77 ± 0.18	[FPS2006] NX 155 (?)
4771 0598	05 39 18.2	–02 29 27	3.02 ± 0.78	...	05 39 18.07	–02 29 28.4	33	Mayrit 634052
4771 0910	05 39 19.5	–02 30 36	2.95 ± 0.68	K3	05 39 18.83	–02 30 53.1	...	Mayrit 596059
R053922–0233	05 39 23.1	–02 33 33	5.46 ± 1.27	K7	05 39 22.86	–02 33 33.0	66	Mayrit 590076
R053930–0238	05 39 30.4	–02 38 20	1.85 ± 0.43	...	05 39 30.56	–02 38 27.0	...	[SWW2004] 222 AB
R053932–0239	05 39 32.7	–02 39 40	3.35 ± 0.74	×	05 39 32.56	–02 39 44.0	44	Mayrit 750107
R053936–0242	05 39 36.4	–02 42 17	16.9 ± 1.42	...	05 39 36.54	–02 42 17.1	8	Mayrit 863116 AB
	05 39 36.8	–02 42 19	14.5 ± 1.26					
R053947–0226	05 39 47.6	–02 26 05	2.54 ± 0.68	...	05 39 47.42	–02 26 16.2	...	Mayrit 1106058
R053947–0232	05 39 47.4	–02 32 22	0.50 ± 0.96	...	05 39 47.84	–02 32 24.9	...	Mayrit 969077

List of Objects

‘ σ Ori’ on page 1
 ‘Horsehead Nebula’ on page 1
 ‘ σ Orionis’ on page 1
 ‘Mayrit 605079’ on page 5
 ‘2E 1456’ on page 6
 ‘UCM0536–0239’ on page 6
 ‘Mayrit 348349’ on page 6
 ‘Mayrit 789281’ on page 6
 ‘Mayrit 863116’ on page 6
 ‘Mayrit 156353’ on page 6
 ‘Mayrit 180277’ on page 6
 ‘Mayrit 403090’ on page 6
 ‘Mayrit 489165’ on page 6
 ‘Mayrit 489196’ on page 6
 ‘Mayrit 397060’ on page 6
 ‘Mayrit 42062’ on page 11
 ‘Mayrit 97212’ on page 11
 ‘Mayrit 344337’ on page 11
 ‘Mayrit 102101’ on page 11
 ‘Mayrit 497054’ on page 11
 ‘Mayrit 433123’ on page 11
 ‘Mayrit 957055’ on page 11
 ‘Mayrit 631045’ on page 11
 ‘Mayrit 662301’ on page 11
 ‘Mayrit 841079’ on page 11
 ‘HH 445’ on page 11
 ‘Mayrit 306125’ on page 13
 ‘Mayrit 189303’ on page 13
 ‘Mayrit 524060’ on page 13
 ‘Mayrit 13084’ on page 13
 ‘Mayrit 182305’ on page 13
 ‘Mayrit 960106’ on page 13
 ‘Mayrit 396273’ on page 13
 ‘Mayrit 487350’ on page 13
 ‘Mayrit 591158’ on page 14
 ‘Mayrit 578123’ on page 14
 ‘Mayrit 521199’ on page 14
 ‘Mayrit 609206’ on page 14

‘Mayrit 332167’ on page 19